



**Max-Planck-Institut  
für Chemische Physik fester Stoffe**

**Max-Planck-Institute  
for Chemical Physics of Solids**



# Determining orbital wavefunctions using core level non-resonant inelastic x-ray scattering

Martin Sundermann<sup>1,2</sup>, Andrea Severing<sup>1,2</sup>, Andrea Amorese<sup>1,2</sup>,  
Hasan Yavas<sup>3</sup>, Hlynur Gretarsson<sup>3</sup>, Maurits Haverkort<sup>4</sup>, Hao Tjeng<sup>1</sup>

<sup>1</sup> *Max-Planck-Institute for Chemical Physics of Solids, Dresden*

<sup>2</sup> *Physics Institute II, University of Cologne*

<sup>3</sup> *DESY – PETRA III – Hamburg*

<sup>4</sup> *Inst. for Theoretical Physics, Heidelberg University*

Theory - calculations

Experiment

← test →

DMFT

Spectroscopy

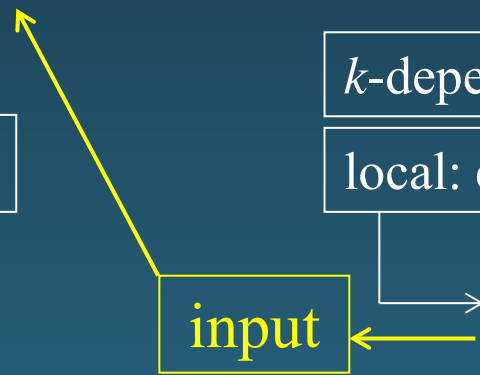
DFT

input

*k*-dependence: e.g. ARPES, neutron

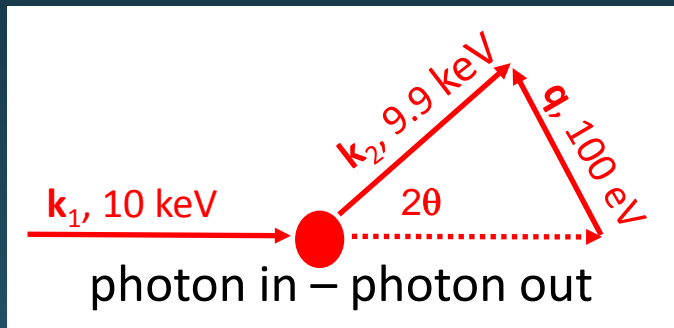
local: e.g. core-level PES/XAS/IXS

on-site correlations, orbitals,  
atomic multiplet structure



# Inelastic x-ray scattering

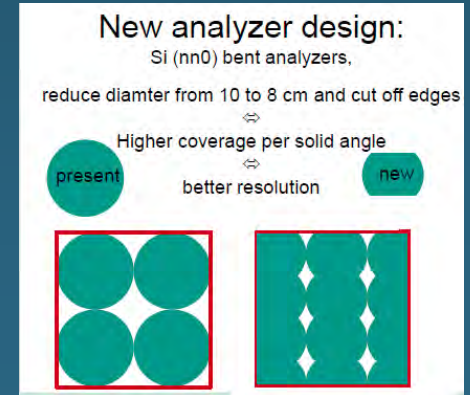
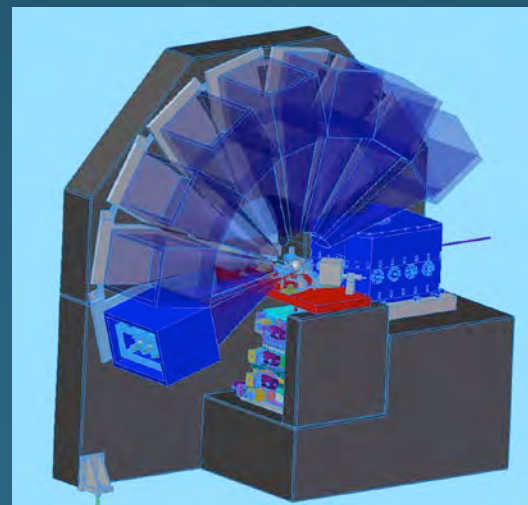
## Max Planck – PETRA III non-resonant inelastic x-ray scattering



- vector-q dependence gives symmetry
- large transferred  $q$  : beyond dipole
  - determination of orbital state
  - spectroscopy and direct imaging

$$S(\mathbf{q}, \omega) = \sum_f |\langle f | e^{i\mathbf{q}\mathbf{r}} | i \rangle|^2 \delta(\hbar\omega_i - \hbar\omega_f - \hbar\omega).$$

- bulk sensitive, extreme conditions



# Non-resonant inelastic x-ray scattering (NIXS) @ N-edge

PHYSICAL REVIEW B 72, 045136 (2005)

one electron theory

## Inelastic scattering from core electrons: A multiple scattering approach

J. A. Soininen,<sup>1,2</sup> A. L. Ankudinov,<sup>2</sup> and J. J. Rehr<sup>2</sup>

<sup>1</sup>*Division of X-ray Physics, Department of Physical Sciences, University of Helsinki, FIN-00014 Finland*

<sup>2</sup>*Department of Physics, University of Washington, Seattle, Washington 98195-1560, USA*

(Received 17 March 2005; published 21 July 2005)

PRL 99, 257401 (2007)

PHYSICAL REVIEW LETTERS

week ending  
21 DECEMBER 2007

## Nonresonant Inelastic X-Ray Scattering Involving Excitonic Excitations: The Examples of NiO and CoO

many body theory

M. W. Haverkort,<sup>1</sup> A. Tanaka,<sup>2</sup> L. H. Tjeng,<sup>1</sup> and G. A. Sawatzky<sup>3</sup>

<sup>1</sup>*II. Physikalisches Institut, Universität zu Köln, Zülpicher Strasse 77, D-50937 Köln, Germany*

<sup>2</sup>*Department of Quantum Matter, ADSM, Hiroshima University, Higashi-Hiroshima 739-8530, Japan*

<sup>3</sup>*Department of Physics and Astronomy, University of British Columbia, Vancouver, British Columbia, Canada V6T 1Z1*

(Received 18 May 2007; published 21 December 2007)



A LETTERS JOURNAL EXPLORING  
THE FRONTIERS OF PHYSICS

January 20

EPL, 81 (2008) 26004

doi: 10.1209/0295-5075/81/26004

[www.epljournal.org](http://www.epljournal.org)

## High multipole transitions in NIXS: Valence and hybridization in 4f systems

R. A. GORDON<sup>1(a)</sup>, G. T. SEIDLER<sup>2</sup>, T. T. FISTER<sup>2</sup>, M. W. HAVERKORT<sup>3</sup>, G. A. SAWATZKY<sup>4</sup>,  
A. TANAKA<sup>5</sup> and T. K. SHAM<sup>6</sup>

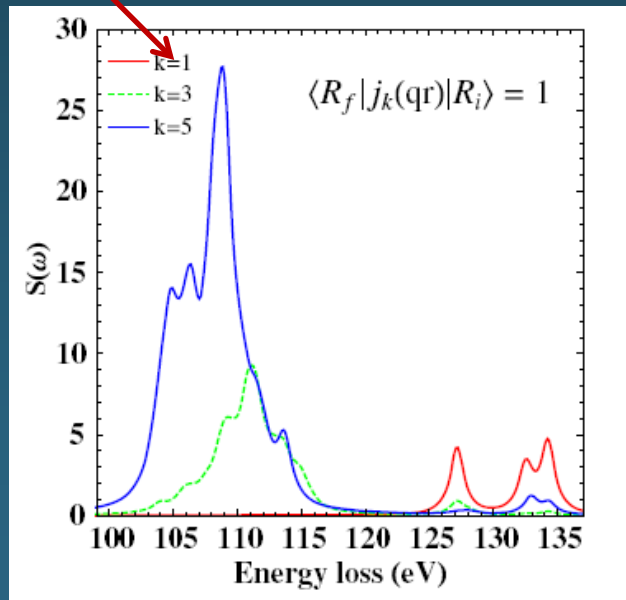
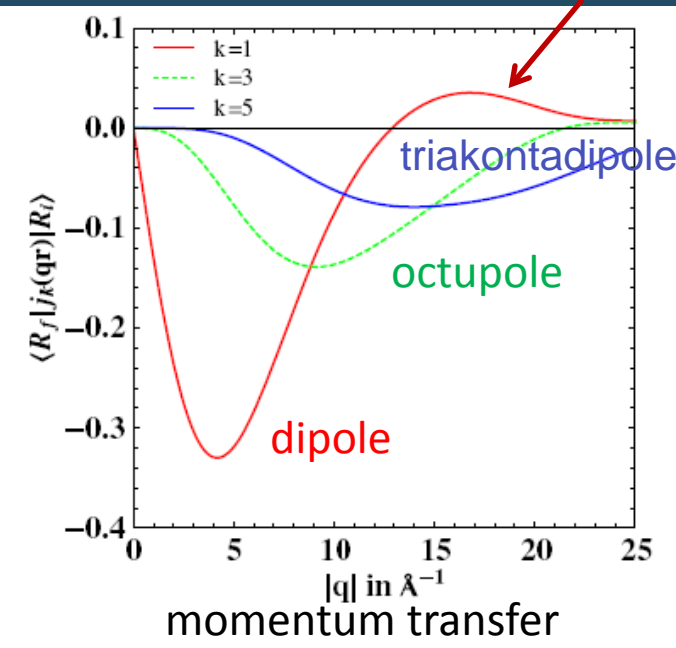
# Non-resonant inelastic x-ray scattering (NIXS) @ N-edge

NIXS is based on:  $q$  dependent multipole selection rules!!

$$S(\mathbf{q}, \omega) = \sum_f |\langle f | e^{i\mathbf{q}\mathbf{r}} | i \rangle|^2 \delta(\hbar\omega_i - \hbar\omega_f - \hbar\omega).$$

$d \rightarrow d$ : monopole, octupole, hexadecapole  
 $d \rightarrow f$  : dipole, octupole, triakontadipole

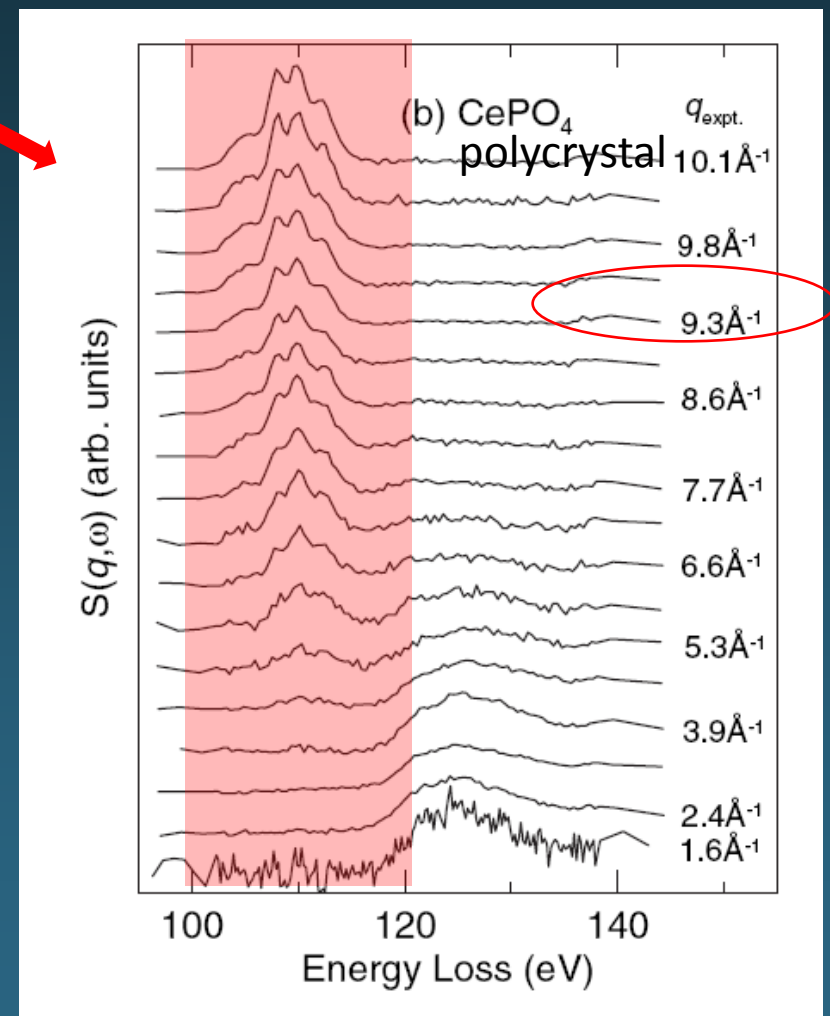
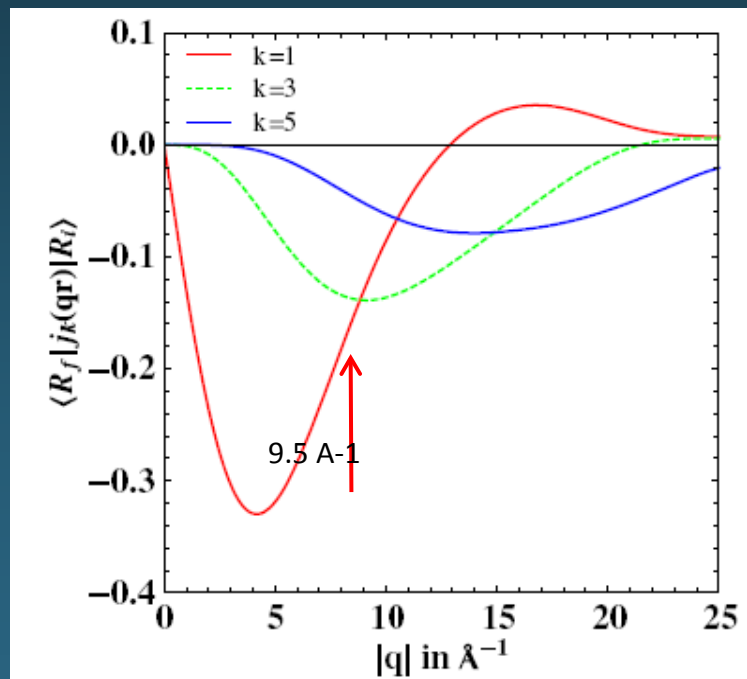
$$S(\mathbf{q}, \omega) = \sum_f \left| \sum_k i^k (2k+1) \underbrace{\langle R_f | j_k(\mathbf{qr}) | R_i \rangle}_{\text{radial}} \times \sum_{m=-k}^k \underbrace{\langle \phi_f | C_{km}^{\hat{\mathbf{q}}} C_{km}^{\hat{\mathbf{r}}} | \phi_i \rangle}_{\text{angular}} \right|^2 \delta(\hbar\omega_i - \hbar\omega_f - \hbar\omega).$$



# Non-resonant inelastic x-ray scattering (NIXS) @ N-edge

## Application to a crystal-field problem at Ce N-edge (4d to 4f)

- The *large*  $|q|$  gives rise to the higher multipole transitions at lower energies !



## **Orientation-dependent x-ray Raman scattering from cubic crystals: natural linear dichroism in MnO and CeO<sub>2</sub>**

**R A Gordon<sup>1</sup>, M W Haverkort<sup>2</sup>, Subhra Sen Gupta<sup>3</sup> and G A Sawatzky<sup>3</sup>**

<sup>1</sup> Dept. of Physics, Simon Fraser University, Burnaby, BC V5A 1S6 Canada

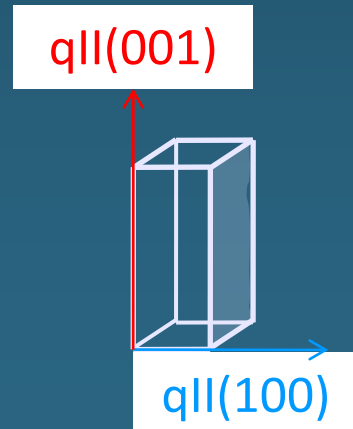
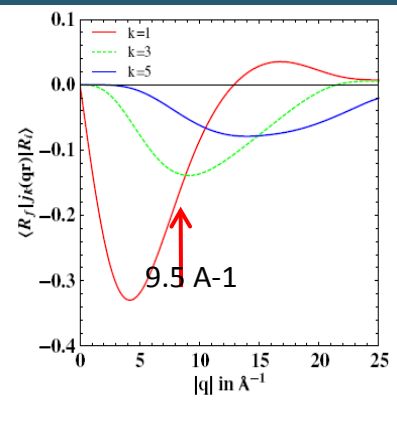
<sup>2</sup> Max Planck Institute for Solid State Research, Heisenbergstr. 1, 70506 Stuttgart, Germany

<sup>3</sup> Dept. of Physics and Astronomy, University of British Columbia, Vancouver, BC V6T 1Z1 Canada

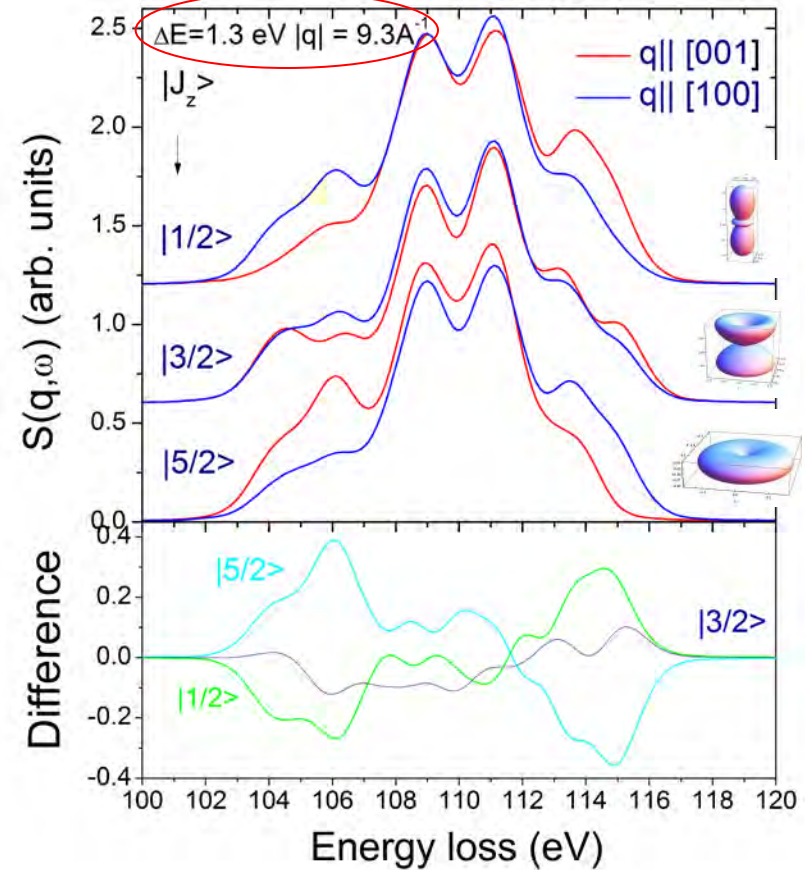
# Non-resonant inelastic x-ray scattering (NIXS) @ N-edge

## Application to a crystal-field problem at Ce N-edge (4d to 4f)

- The *large*  $|q|$  gives rise to the higher multipole transitions.
- Vector  $q$  dependence on a *single crystal* should give sensitivity to orbital anisotropies ( $J_z$  admixture) in analogy to polarization dependence in XAS.
- Simulate NIXS for pure  $J_z$  states for vector  $q$  "in-plane" and "out-of-plane" at large  $|q|$  at the Ce N-edge ( $4d \rightarrow 4f$ ) [code by M.W. Haverkort]



### Simulation NIXS N-edge



# Non-resonant inelastic x-ray scattering (NIXS) @ N-edge

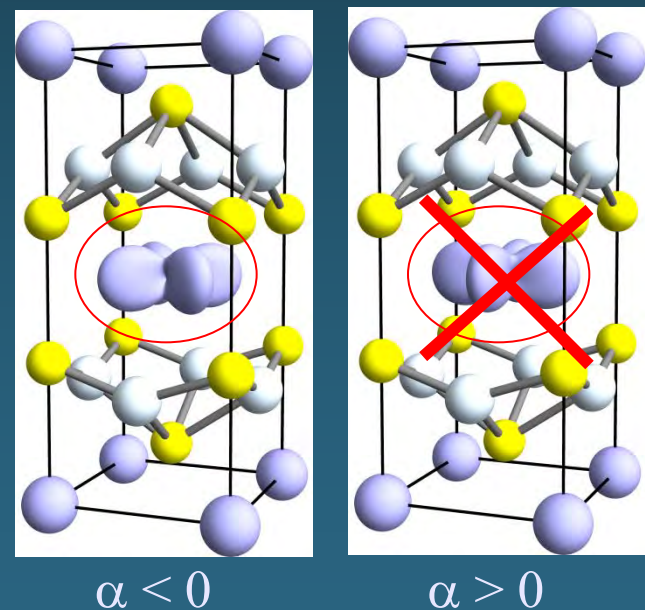
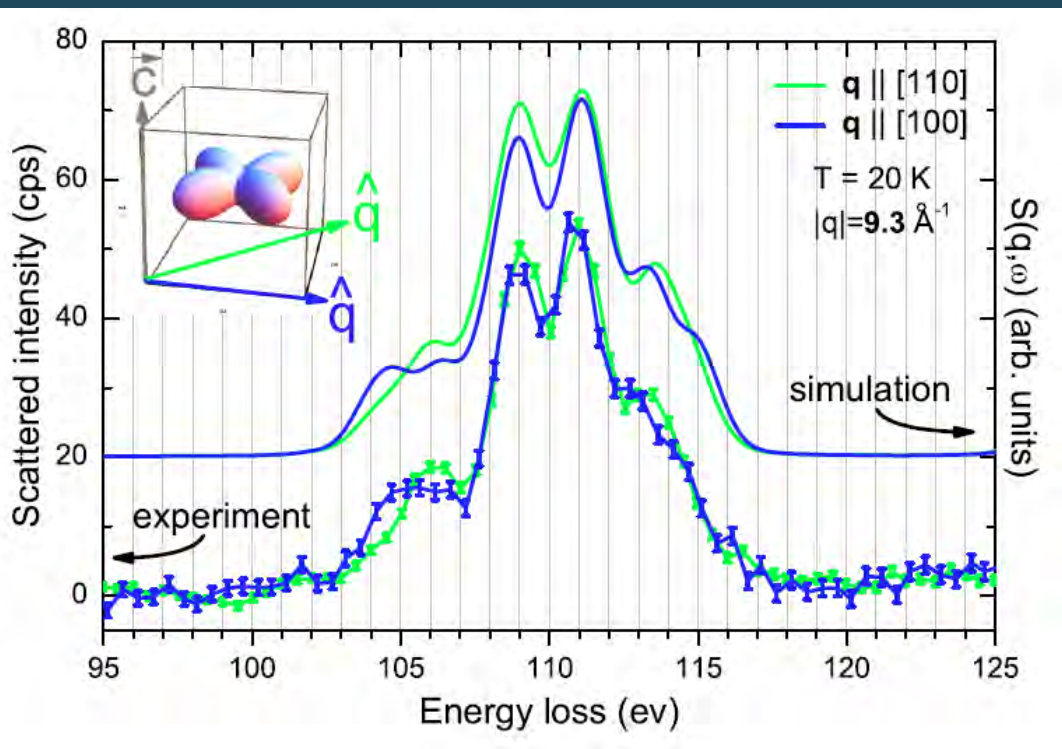
PRL 109, 046401 (2012)

PHYSICAL REVIEW LETTERS

week ending  
27 JULY 2012

## Determining the In-Plane Orientation of the Ground-State Orbital of $\text{CeCu}_2\text{Si}_2$

T. Willers,<sup>1</sup> F. Strigari,<sup>1</sup> N. Hiraoka,<sup>2</sup> Y. Q. Cai,<sup>3</sup> M. W. Haverkort,<sup>4</sup> K.-D. Tsuei,<sup>2</sup> Y. F. Liao,<sup>2</sup> S. Seiro,<sup>5</sup> C. Geibel,<sup>5</sup> F. Steglich,<sup>5</sup> L. H. Tjeng,<sup>5</sup> and A. Severing<sup>1</sup>



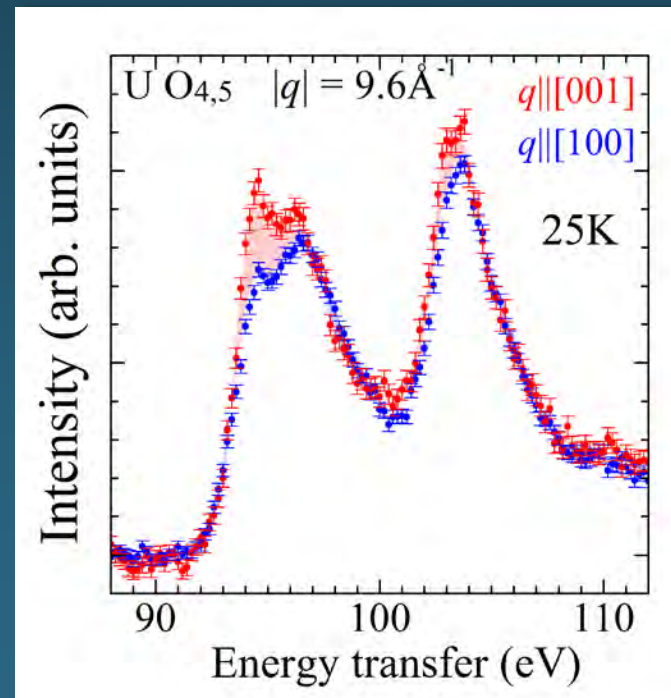
# Direct bulk-sensitive probe of 5f symmetry in $\text{URu}_2\text{Si}_2$

Martin Sundermann<sup>a</sup>, Maurits W. Haverkort<sup>b,1</sup>, Stefano Agrestini<sup>b</sup>, Ali Al-Zein<sup>c,2</sup>, Marco Moretti Sala<sup>c</sup>, Yingkai Huang<sup>d</sup>, Mark Golden<sup>d</sup>, Anne de Visser<sup>d</sup>, Peter Thalmeier<sup>b</sup>, Liu Hao Tjeng<sup>b</sup>, and Andrea Severing<sup>a,3</sup>

<sup>a</sup>Institute of Physics II, University of Cologne, 50937 Cologne, Germany; <sup>b</sup>Max-Planck-Institute for Chemical Physics of Solids, 01187 Dresden, Germany;

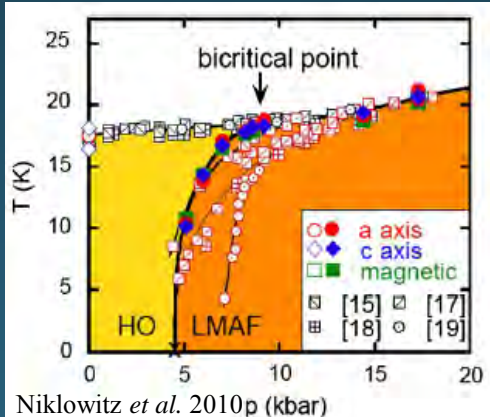
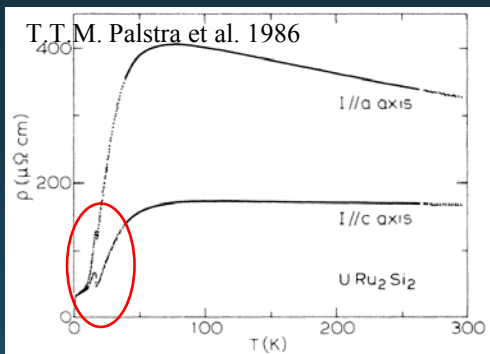
<sup>c</sup>European Synchrotron Radiation Facility, 38043 Grenoble Cédex, France; and <sup>d</sup>Van der Waals-Zeeman Institute, University of Amsterdam, 1098 XH Amsterdam, The Netherlands

ID20 NIXS



# URu<sub>2</sub>Si<sub>2</sub> and the hidden order state

T.T.M. Palstra *et al.* 1985, W. Schlabitz *et al.* 1986, M.B. Maple *et al.* 1986



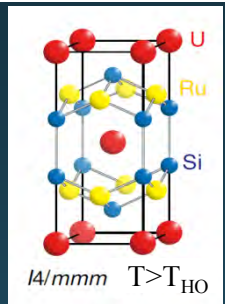
Amitsuka *et al.* 2007, Niklowitz *et al.* 2010

Meng. *et al.* 2013, Bareille *et al.* 2014, Chatterjee *et al.* 2013, Okazaki *et al.* 2011, Tonegawa *et al.* 2014

Hassinger *et al.* 2010, Park *et al.* 2012, Meng *et al.* 2013, Barleile *et al.* 2014, Aynajian *et al.* 2010, Schmidt *et al.* 2010, Broholm *et al.* 1991, Wiebe *et al.* 2007, Buhot *et al.* 2014, Kung *et al.* 2015, Bourdarot *et al.* 2010

## Phase diagram

- $T_{HO} = 17.5 \text{ K}$
- $T_{sc} = 1.5 \text{ K}$
- $T < T_{HO}$  small  $\mu_{ord} \Leftrightarrow$  parasitic minority phase
- $p \geq 0.7 \text{ GPa}$  af  $T_N \approx T_{HO}$  (*LMAF*-phase)



## HO phase

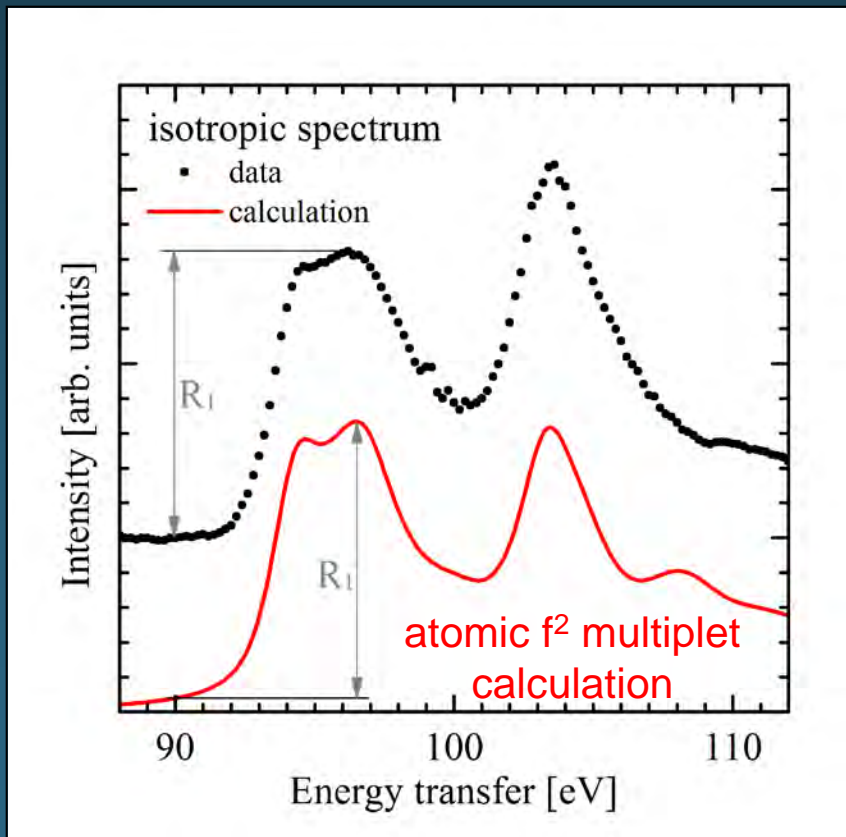
- 2<sup>nd</sup> order phase transition  $\Leftrightarrow$  into electronically ordered state
- large loss of entropy ( $\approx 1/5 \ln 2$ )
- Fermi surface reconstruction
- change of quasiparticle scattering rate
- Fermi surfaces of *HO*  $\approx$  Fermi surface *LMAF* phase
- Loss of fourfold symmetry

## Energy scales

- $\Delta_{hyb} \approx 13 \text{ meV}$  (150K) opening at  $T_{hyb} \approx 27 \text{ K} > T_{HO}$
- $\Delta_{HO} \approx 4 \text{ meV}$  (45K) in charge and spin channel
- $\Delta_{res} \approx 1.6 \text{ meV}$  (18K) in charge and spin channel

# Non-resonant inelastic scattering $\text{U } 5\text{d} \rightarrow 5\text{f}$ of $\text{URu}_2\text{Si}_2$

Isotropic spectrum sum of  
all CF states



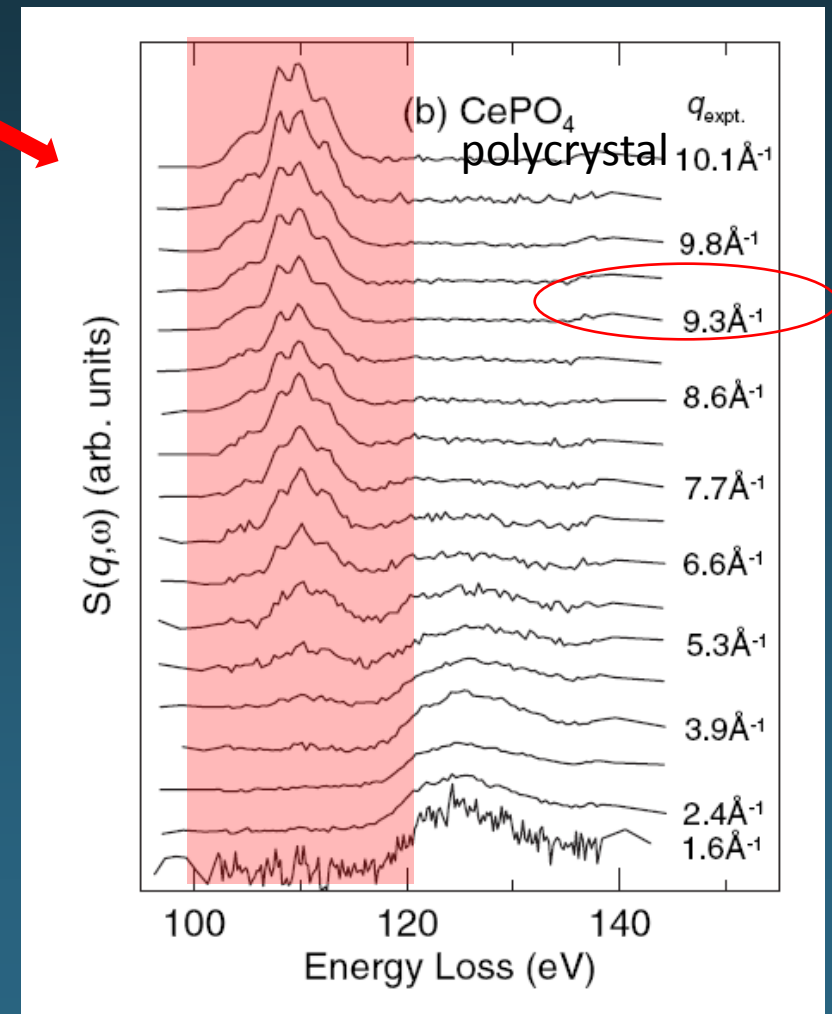
- Spin orbit and Coulomb interaction for localized  $\text{U}^{4+} f^2$  always yield  $J = 4$ .
- Atomic values Cowan code
- Adjust here reduction factors ( $5f-5f$  and  $5d-5f \approx 50\%$ )
- Relative contributions of spin-orbit and Coulomb interaction determine ratio of  $L=3,4,5$  (here 1%, 14% and 85 %).
- FWHM = 0.8 eV Gaussian for resolution  
FWHM = 1.3 eV Lorenzian for lifetime
- Simulation by *Quenty – Haverkort*

# Non-resonant inelastic x-ray scattering (NIXS) @ N-edge

## Application to a crystal-field problem at Ce N-edge (4d to 4f)

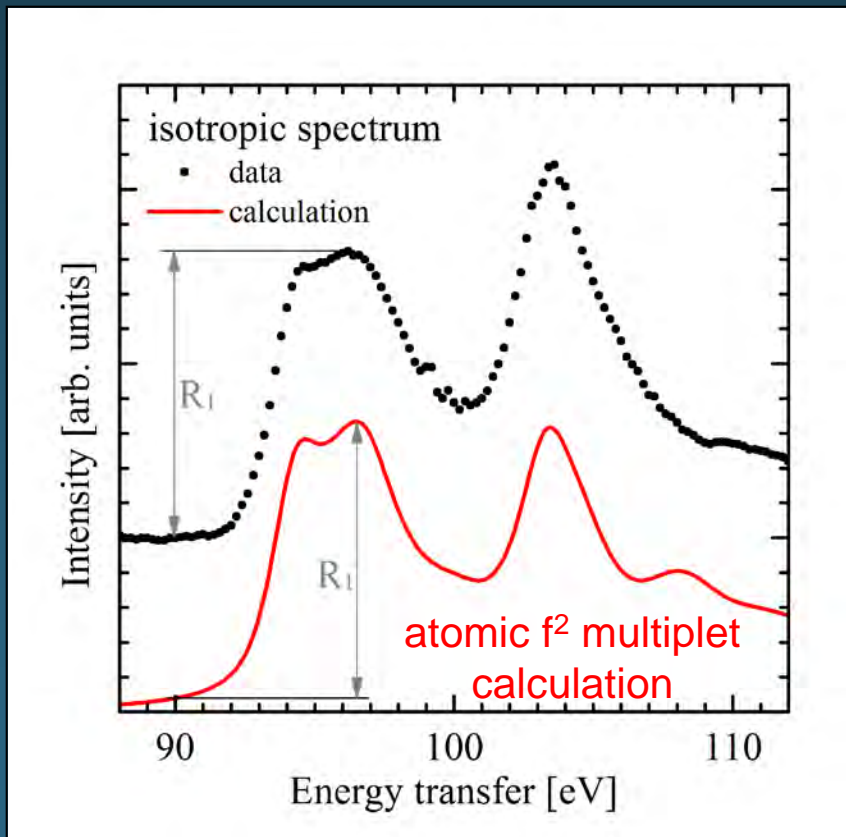
- The *large*  $|q|$  gives rise to the higher multipole transitions at lower energies !

Further away from continuum states  
→ more excitonic !



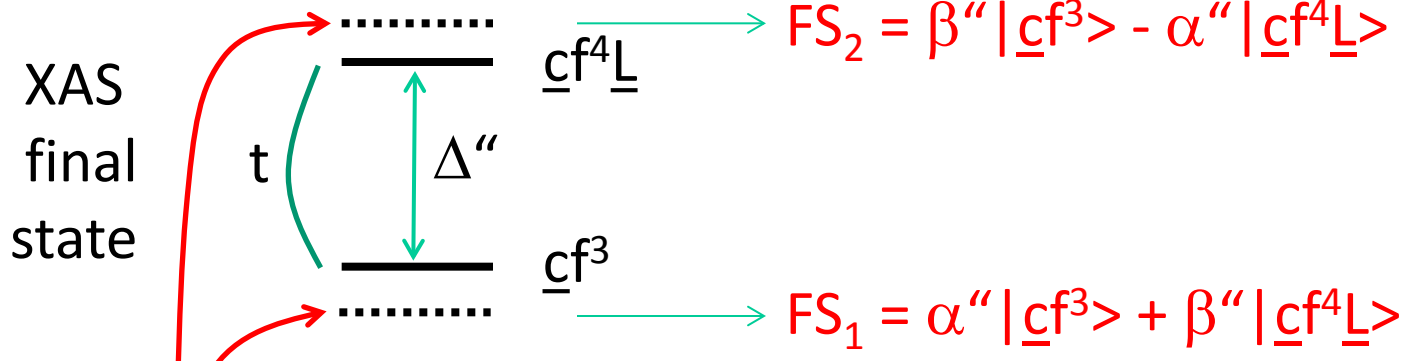
# Non-resonant inelastic scattering $\text{U } 5\text{d} \rightarrow 5\text{f}$ of $\text{URu}_2\text{Si}_2$

Isotropic spectrum sum of  
all CF states

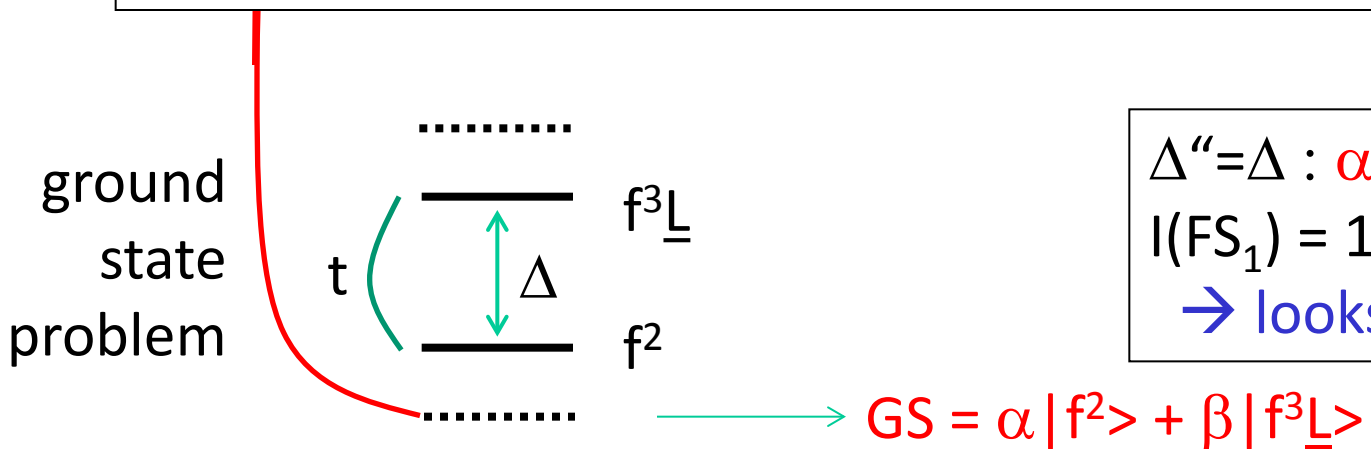


- Spin orbit and Coulomb interaction for localized  $\text{U}^{4+} f^2$  always yield  $J = 4$ .
- Atomic values Cowan code
- Adjust here reduction factors ( $5f-5f$  and  $5d-5f \approx 50\%$ )
- Relative contributions of spin-orbit and Coulomb interaction determine ratio of  $L=3,4,5$  (here 1%, 14% and 85 %).
- FWHM = 0.8 eV Gaussian for resolution  
FWHM = 1.3 eV Lorenzian for lifetime
- Simulation by *Quenty – Haverkort*

$$\begin{aligned}
 I(FS_2) &= |\langle FS_2 | f^+ c | GS \rangle|^2 \\
 &= |\beta'' \langle \underline{c}f^3 | -\alpha'' \langle \underline{c}f^4 \underline{L} | f^+ c | \alpha | f^2 \rangle + \beta | f^3 \underline{L} \rangle|^2 = |\beta'' \alpha - \alpha'' \beta|^2
 \end{aligned}$$



$$\begin{aligned}
 I(FS_1) &= |\langle FS_1 | f^+ c | GS \rangle|^2 \\
 &= |\alpha'' \langle \underline{c}f^3 | + \beta'' \langle \underline{c}f^4 \underline{L} | f^+ c | \alpha | f^2 \rangle + \beta | f^3 \underline{L} \rangle|^2 = |\alpha'' \alpha + \beta'' \beta|^2
 \end{aligned}$$



$\Delta'' = \Delta : \alpha'' = \alpha, \beta'' = \beta \rightarrow$   
 $I(FS_1) = 1 \quad I(FS_2) = 0$   
 $\rightarrow \text{looks like ionic !}$

## XAS ( $d \rightarrow f$ ) final state: e.g. Uranium M-edges

Diagram illustrating the energy levels for the XAS final state ( $\underline{c}\underline{f}^{n+2}\underline{L}$ ). The initial state is  $\underline{c}\underline{f}^{n+1}$ . A green double-headed arrow between them is labeled  $\Delta''$ . The energy equation is:

$$E(\underline{c}\underline{f}^{n+2}\underline{L}) = (n+2)E_f + \frac{1}{2}(n+2)(n+1)U_{ff} - E_L + E_c - (n+2)U_{cf}$$


---


$$E(\underline{c}\underline{f}^{n+1}) = (n+1)E_f + \frac{1}{2}(n+1)nU_{ff} + E_c - (n+1)U_{cf}$$

$$\Delta'' = E(\underline{c}\underline{f}^{n+2}\underline{L}) - (\underline{c}\underline{f}^n) = \Delta + U_{ff} - U_{cf}$$

$U_{ff} \sim U_{cf} \rightarrow \Delta'' \sim \Delta \rightarrow XAS \sim \text{ionic}$

## ground state problem

Diagram illustrating the energy levels for the ground state problem. The initial state is  $f^n$ . The final state is  $f^{n+1}\underline{L}$ . A green double-headed arrow between them is labeled  $\Delta$ . The energy equation is:

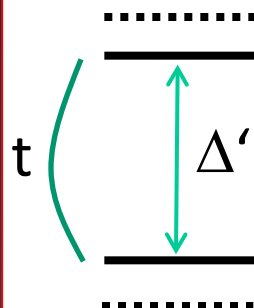
$$E(f^{n+1}\underline{L}) = (n+1)E_f + \frac{1}{2}(n+1)nU_{ff} - E_L$$


---


$$E(f^n) = nE_f + \frac{1}{2}n(n-1)U_{ff}$$

$$\Delta = E(f^{n+1}\underline{L}) - (f^n) = E_f - E_L + nU_{ff}$$

## XPS final state

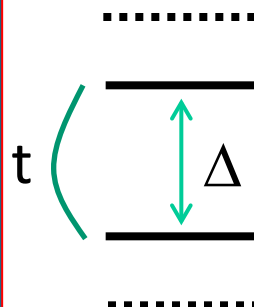

$$\begin{array}{lll} \text{cf}^{n+1}\underline{\text{L}} & E(\text{cf}^{n+1}\underline{\text{L}}) = (n+1)E_f + \frac{1}{2}(n+1)nU_{ff} - E_L + E_c - (n+1)U_{cf} \\ \text{cf}^n & E(\text{cf}^n) = nE_f + \frac{1}{2}n(n-1)U_{ff} + E_c - nU_{cf} \end{array}$$

---

$$\Delta' = E(\text{cf}^{n+1}\underline{\text{L}}) - (\text{cf}^n) = \Delta - U_{cf}$$

**Δ' is very different from Δ → XPS : satellites !**

## ground state problem


$$\begin{array}{lll} \text{f}^{n+1}\underline{\text{L}} & E(\text{f}^{n+1}\underline{\text{L}}) = (n+1)E_f + \frac{1}{2}(n+1)nU_{ff} - E_L \\ \text{f}^n & E(\text{f}^n) = nE_f + \frac{1}{2}n(n-1)U_{ff} \end{array}$$

---

$$\Delta = E(\text{f}^{n+1}\underline{\text{L}}) - (\text{f}^n) = E_f - E_L + nU_{ff}$$

## XAS ( $p \rightarrow d$ ) final state: e.g. Uranium L-edges

The diagram shows two energy levels. The upper level is labeled  $\underline{cd}^1f^{n+1}\underline{L}$  and the lower level is labeled  $\underline{cd}^1f^n$ . A green double-headed arrow between them is labeled  $\Delta'''$ . To the left of the levels, the letter 't' is written vertically.

$$\begin{aligned} E(\underline{cd}^1f^{n+1}\underline{L}) &= (n+1)E_f + \frac{1}{2}(n+1)nU_{ff} - E_L + E_c + E_d - \\ &\quad (n+1)U_{cf} - U_{cd} + (n+1)U_{df} \\ E(\underline{cd}^1f^n) &= nE_f + \frac{1}{2}n(n-1)U_{ff} + E_c + E_d - nU_{cf} - U_{cd} + nU_{df} \end{aligned}$$


---


$$\Delta''' = E(\underline{cd}^1f^{n+1}\underline{L}) - (\underline{cd}^1f^n) = \Delta - U_{cf} + U_{df}$$

$U_{df} \sim 0 \rightarrow \Delta''' \sim \Delta' \rightarrow L\text{-XAS} \sim XPS$

## ground state problem

The diagram shows two energy levels. The upper level is labeled  $f^{n+1}\underline{L}$  and the lower level is labeled  $f^n$ . A green double-headed arrow between them is labeled  $\Delta$ . To the left of the levels, the letter 't' is written vertically.

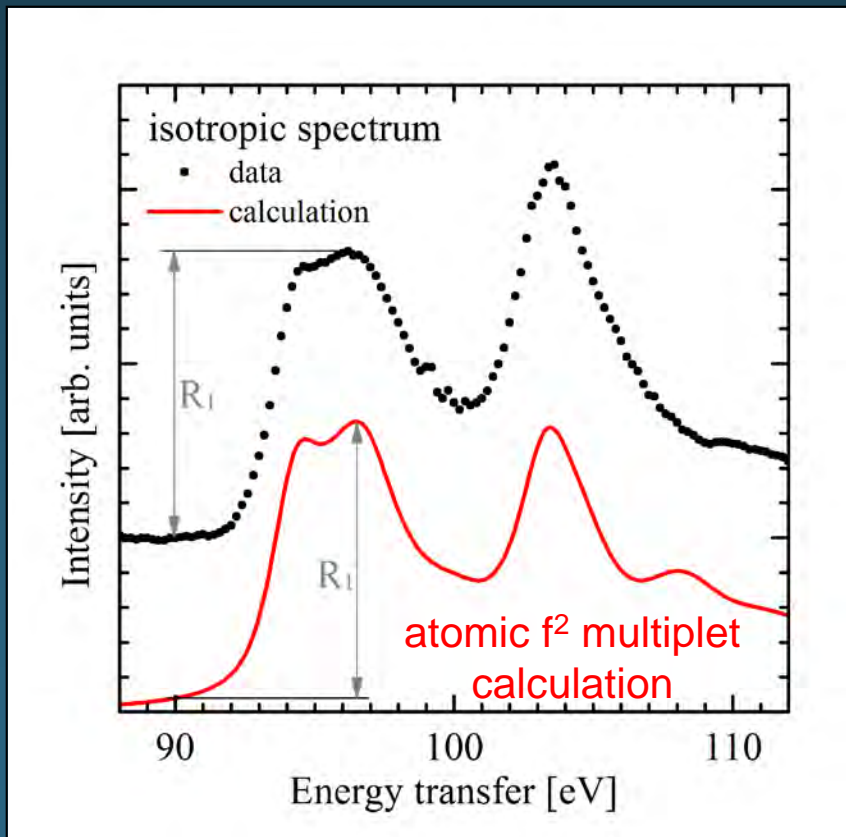
$$\begin{aligned} E(f^{n+1}\underline{L}) &= (n+1)E_f + \frac{1}{2}(n+1)nU_{ff} - E_L \\ E(f^n) &= nE_f + \frac{1}{2}n(n-1)U_{ff} \end{aligned}$$


---

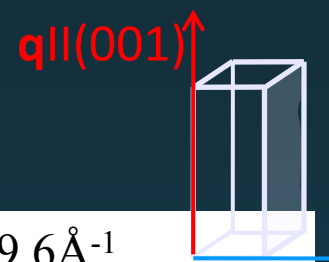

$$\Delta = E(f^{n+1}\underline{L}) - (f^n) = E_f - E_L + nU_{ff}$$

# Non-resonant inelastic scattering $\text{U } 5\text{d} \rightarrow 5\text{f}$ of $\text{URu}_2\text{Si}_2$

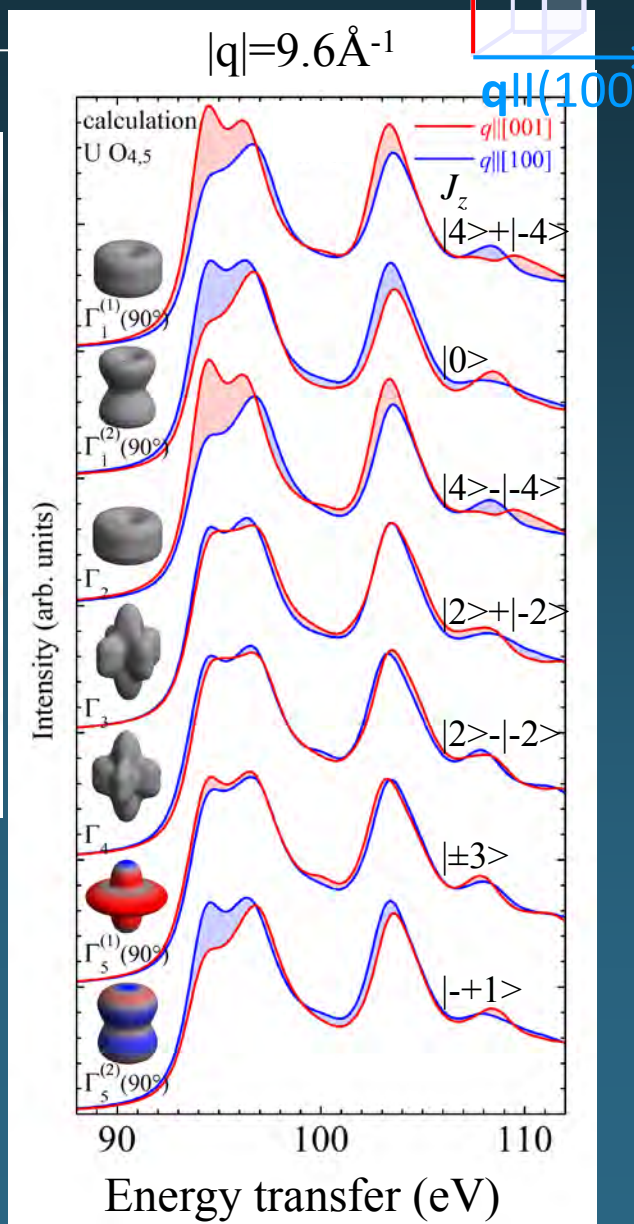
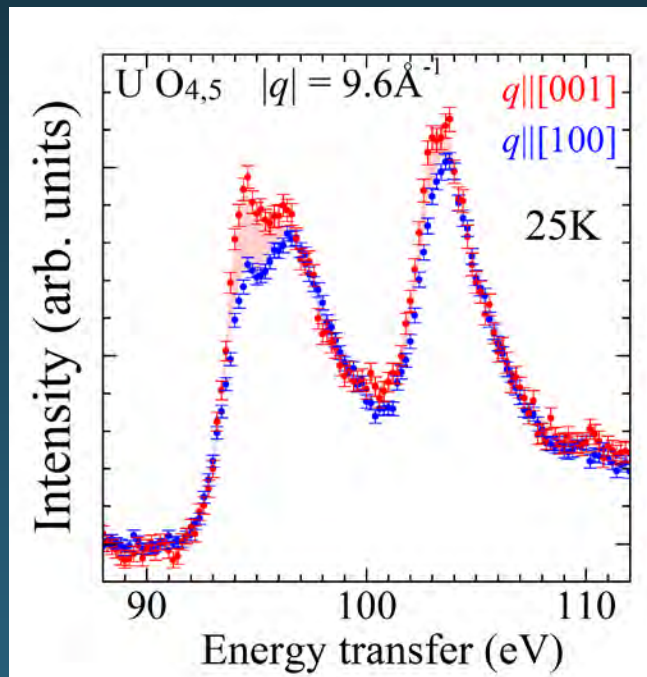
Isotropic spectrum sum of  
all CF states

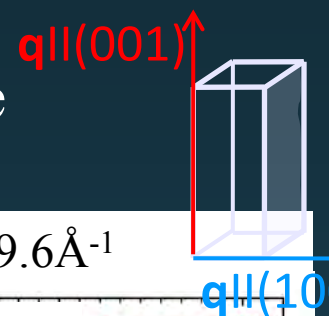


- Spin orbit and Coulomb interaction for localized  $\text{U}^{4+} f^2$  always yield  $J = 4$ .
- Atomic values Cowan code
- Adjust here reduction factors ( $5f-5f$  and  $5d-5f \approx 50\%$ )
- Relative contributions of spin-orbit and Coulomb interaction determine ratio of  $L=3,4,5$  (here 1%, 14% and 85 %).
- FWHM = 0.8 eV Gaussian for resolution  
FWHM = 1.3 eV Lorenzian for lifetime
- Simulation by *Quenty – Haverkort*



## NIXS: groundstate $T > T_{HO}$





# Simulation of spectra with full multiplet routine

*Quany by M.W. Haverkort*

$J = 4, J_z = \{-4, -3, \dots, 2, 3, 4\}$   
 tetragonal CEF splits  $J = 4$   
 into five singlets and 2 doublets

$$\Gamma_1^{(1)}(\theta) = \cos(\theta) |0\rangle + \sin(\theta) \sqrt{\frac{1}{2}} (|4\rangle + |-4\rangle)$$

$$\Gamma_1^{(2)}(\theta) = \sin(\theta) |0\rangle - \cos(\theta) \sqrt{\frac{1}{2}} (|4\rangle + |-4\rangle)$$

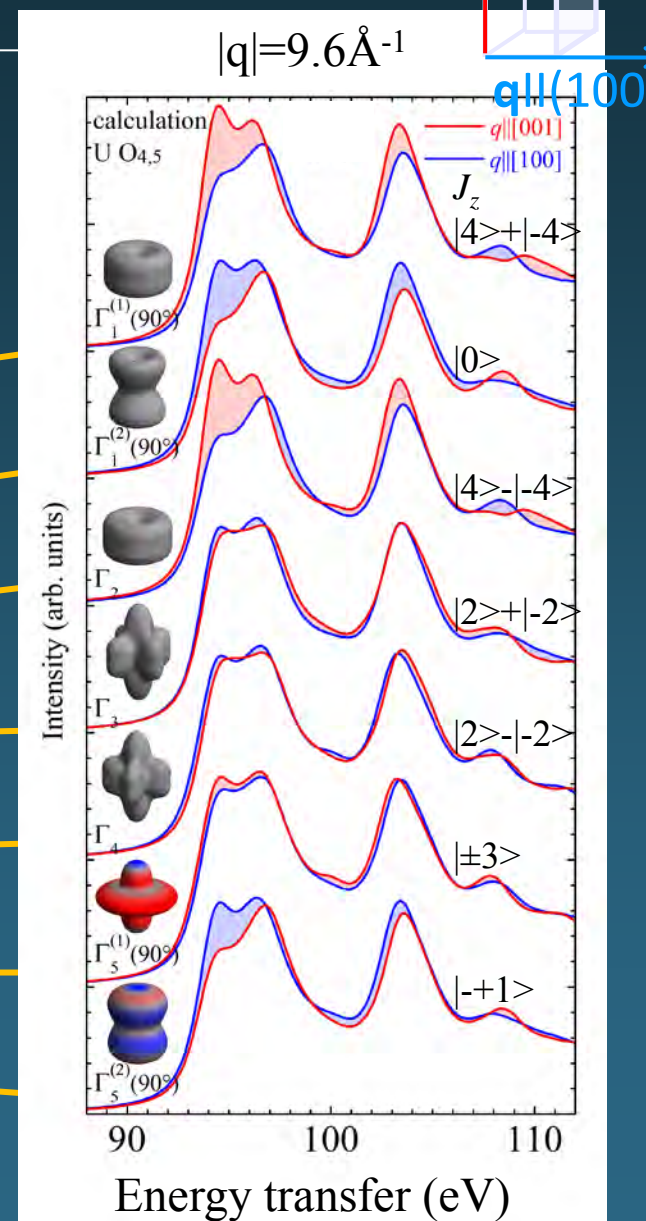
$$\Gamma_2 = \sqrt{\frac{1}{2}} (|4\rangle - |-4\rangle)$$

$$\Gamma_3 = \sqrt{\frac{1}{2}} (|2\rangle + |-2\rangle)$$

$$\Gamma_4 = \sqrt{\frac{1}{2}} (|2\rangle - |-2\rangle)$$

$$\Gamma_5^{(1)}(\phi) = \cos(\phi) |\mp 1\rangle + \sin(\phi) |\pm 3\rangle$$

$$\Gamma_5^{(2)}(\phi) = \sin(\phi) |\mp 1\rangle - \cos(\phi) |\pm 3\rangle$$



$$U^{4+} f^2$$

$J = 4, J_z = \{-4, -3, \dots, 2, 3, 4\}$   
 tetragonal CEF splits  $J = 4$   
 into five singlets and 2 doublets

Some ground state suggestions

$$\Gamma_1^{(1)}(\theta) = \cos(\theta) |0\rangle + \sin(\theta) \sqrt{\frac{1}{2}} (|4\rangle + |-4\rangle)$$

$$\Gamma_1^{(2)}(\theta) = \sin(\theta) |0\rangle - \cos(\theta) \sqrt{\frac{1}{2}} (|4\rangle + |-4\rangle)$$

$$\Gamma_2 = \sqrt{\frac{1}{2}} (|4\rangle - |-4\rangle)$$

$$\Gamma_3 = \sqrt{\frac{1}{2}} (|2\rangle + |-2\rangle)$$

$$\Gamma_4 = \sqrt{\frac{1}{2}} (|2\rangle - |-2\rangle)$$

$$\Gamma_5^{(1)}(\phi) = \cos(\phi) |\mp 1\rangle + \sin(\phi) |\pm 3\rangle$$

$$\Gamma_5^{(2)}(\phi) = \sin(\phi) |\mp 1\rangle - \cos(\phi) |\pm 3\rangle$$

Nieuwenhuys *et al.* (1987), Yanagisawa *et al.* (2013), Kiss & Fazekas (2005), Kusunose *et al.* (2011), Hanzawa (2012)

Haule & Kotliar (2009)

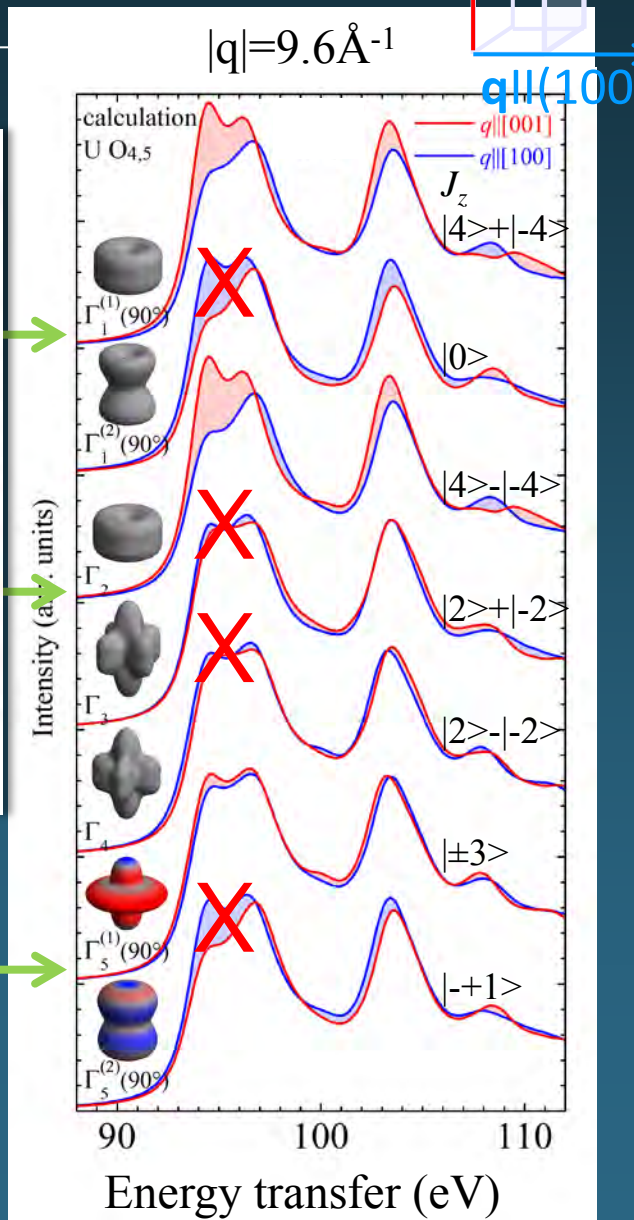
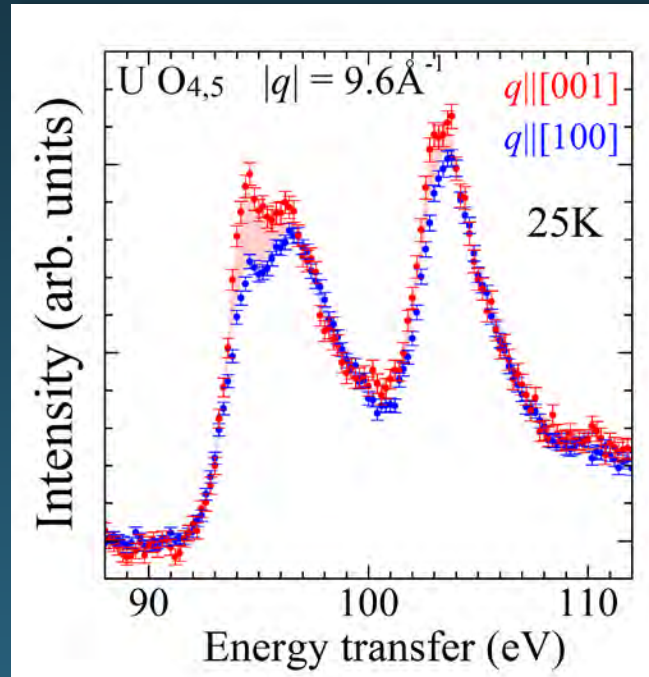
Santini & Amoretti (1994), Nagao & Igarashi (2005)

Nagao & Igarashi (2005), Kuwahara *et al.* (1997)

Nagao & Igarashi (2005), Ohkawa & Shimizu (1999), Chandra *et al.* (2013), Wray *et al.* (2015)

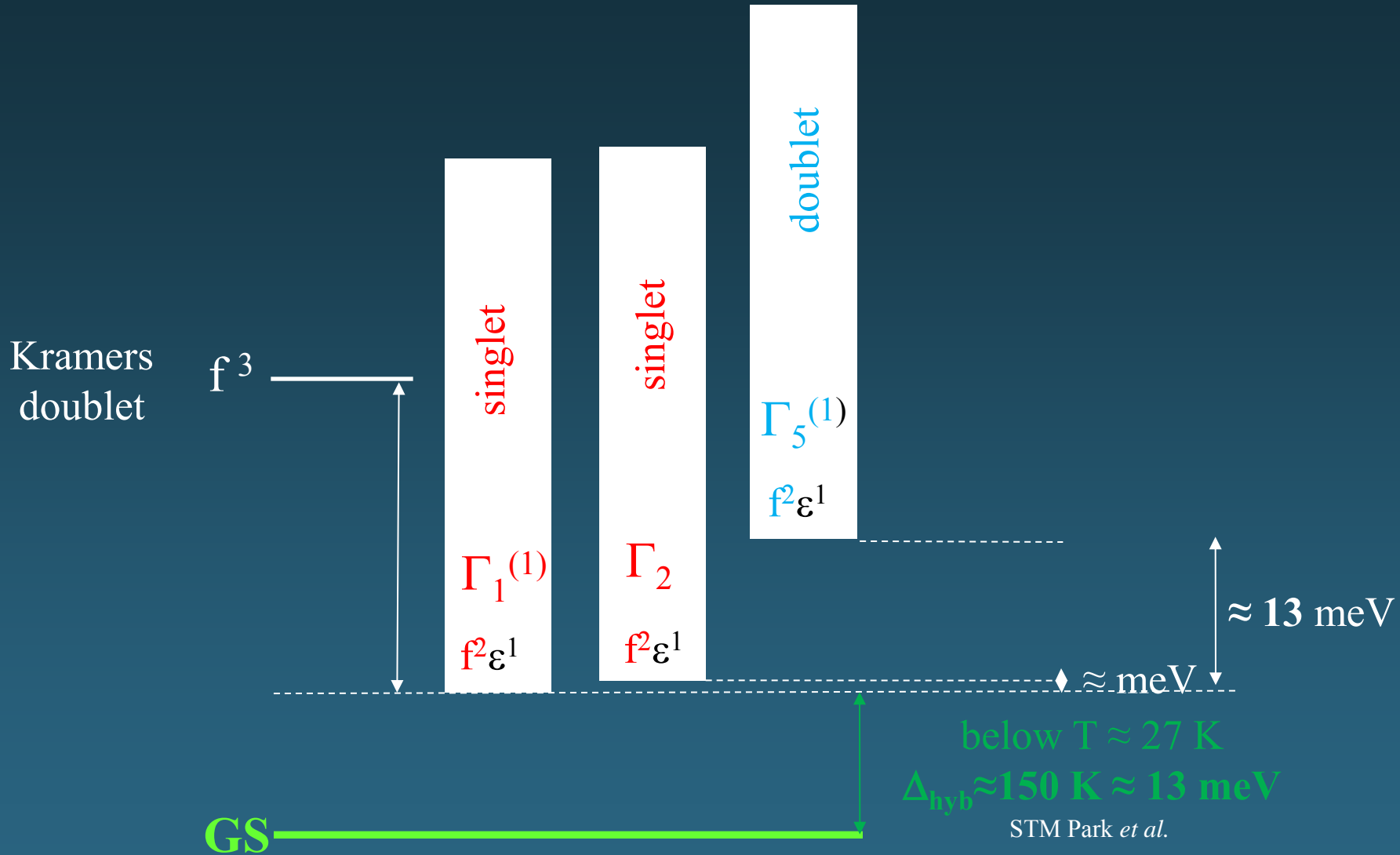
Ohkawa & Shimizu (1999), Sugiyama *et al.* (1999), Chandra *et al.* (2013),

# NIXS: groundstate $T > T_{HO}$



GS: mainly singlet  $\Gamma_1^{(1)}$  ( $\approx 90^\circ$ ) and/or  $\Gamma_2$  and some other state, e.g. the doublet  $\Gamma_5^{(1)}$  ( $\approx 90^\circ$ ) mixed in.

# How to set up the energy level diagram of URu<sub>2</sub>Si<sub>2</sub> ??



GS: mainly singlet  $\Gamma_1^{(1)}$ ( $\approx 90^\circ$ ) and/or  $\Gamma_2$  and some other state e.g. the doublet  $\Gamma_5^{(1)}$ ( $\approx 90^\circ$ ) mixed in.

## Topological Kondo Insulators

Maxim Dzero,<sup>1</sup> Kai Sun,<sup>1</sup> Victor Galitski,<sup>1</sup> and Piers Coleman<sup>2</sup>

<sup>1</sup>*Joint Quantum Institute and Department of Physics, University of Maryland, College Park, Maryland 20742, USA*

<sup>2</sup>*Center for Materials Theory, Rutgers University, Piscataway, New Jersey 08854, USA*

(Received 22 December 2009; published 12 March 2010)

ISSN 1063-7761, Journal of Experimental and Theoretical Physics, 2013, Vol. 117, No. 3, pp. 499–507. © Pleiades Publishing, Inc., 2013.

## A New Exotic State in an Old Material: a Tale of SmB<sub>6</sub><sup>1</sup>

M. Dzero<sup>a</sup> and V. Galitski<sup>b</sup>

<sup>a</sup> *Department of Physics, Kent State University, Kent, OH 44242 USA*

<sup>b</sup> *Condensed Matter Theory Center and Department of Physics, University of Maryland, College Park, MD 20742 USA*

e-mail: galitski@physics.umd.edu

Received April 26, 2013

topological insulator in higher orbital systems. The special attention is given to the already existing *f*-orbital materials [30], such as CeNiSn, Ce<sub>3</sub>Bi<sub>4</sub>Pt<sub>3</sub>, YbB<sub>12</sub>, and SmB<sub>6</sub>. These materials, which are called Kondo insulators, have all the necessary features needed for realizing topological behavior: strong spin–orbit coupling, strong electron–electron interactions, and orbitals with opposite parity (see table).

# Topological Kondo Insulators

Maxim Dzero,<sup>1,2</sup> Jing Xia,<sup>3</sup> Victor Galitski,<sup>4,5</sup>  
and Piers Coleman<sup>6,7</sup>

Annu. Rev. Condens. Matter Phys. 2016. 7:249–80

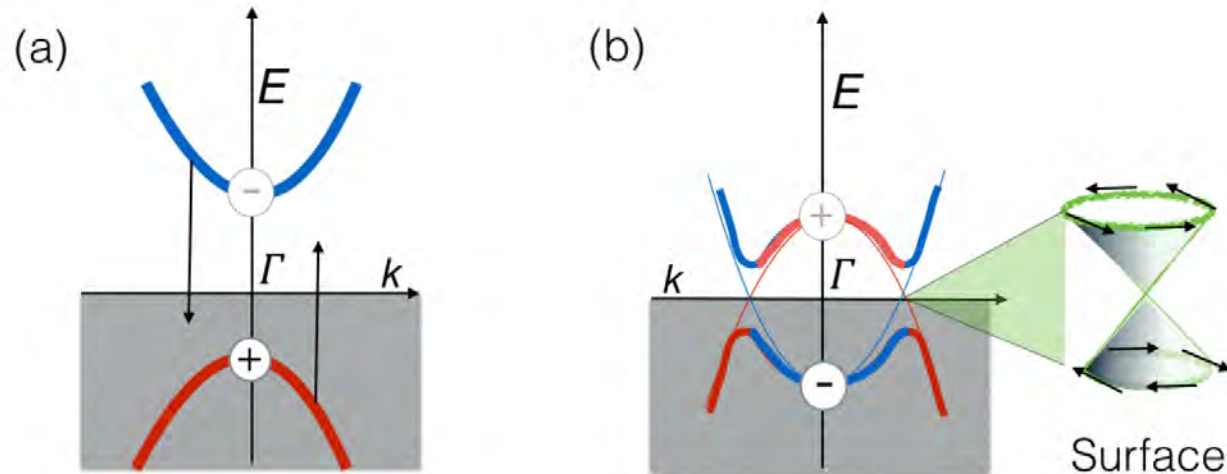


**Figure 3**

Showing (a) topologically trivial band insulator with  $Z_2 = +1$  (b) band-crossing of even and odd parity states at an odd number of high symmetry points leads to a topological insulator with  $Z_2 = -1$ . Each band crossing generates a Dirac cone of spin-momentum locked surface states.

# Topological Kondo Insulators

Maxim Dzero,<sup>1,2</sup> Jing Xia,<sup>3</sup> Victor Galitski,<sup>4,5</sup>  
and Piers Coleman<sup>6,7</sup>

Annu. Rev. Condens. Matter Phys. 2016. 7:249–80

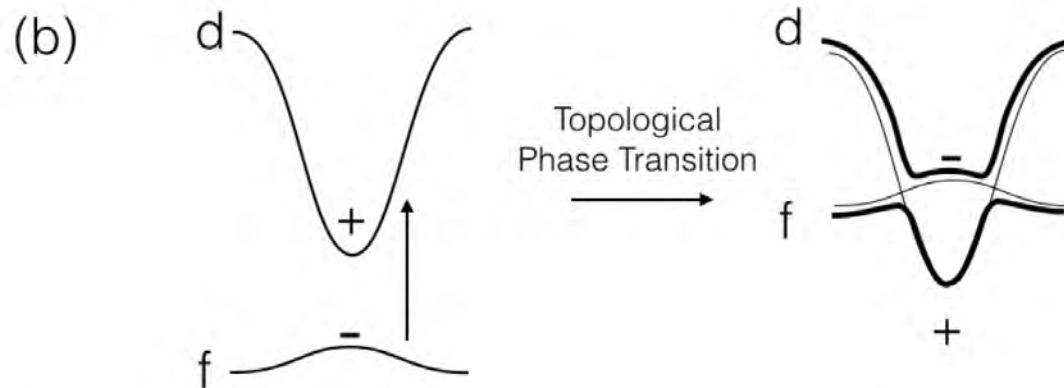


**Figure 4**

(a) If we ignore the effects of topology in a conventional Kondo insulator, the interaction can be turned on adiabatically. When the interactions are turned on, the lower band is pushed into the upper band. Two bands of the same parity will always repel one-another and will not cross when the interactions are turned on. (b) When interactions are turned on in a topological insulator, they can lead to band-crossing and a topological phase transition. Here, interactions cause an f-band to push up into a d-band. Since the two bands have opposite parity, they do not hybridize at the high symmetry point so band-crossing occurs, leading to a topological phase transition.

always finite resistivity,  
even in purest samples

metallic surface states,  
topologically protected ?!

J. Denlinger et al., arXiv:1312.6637

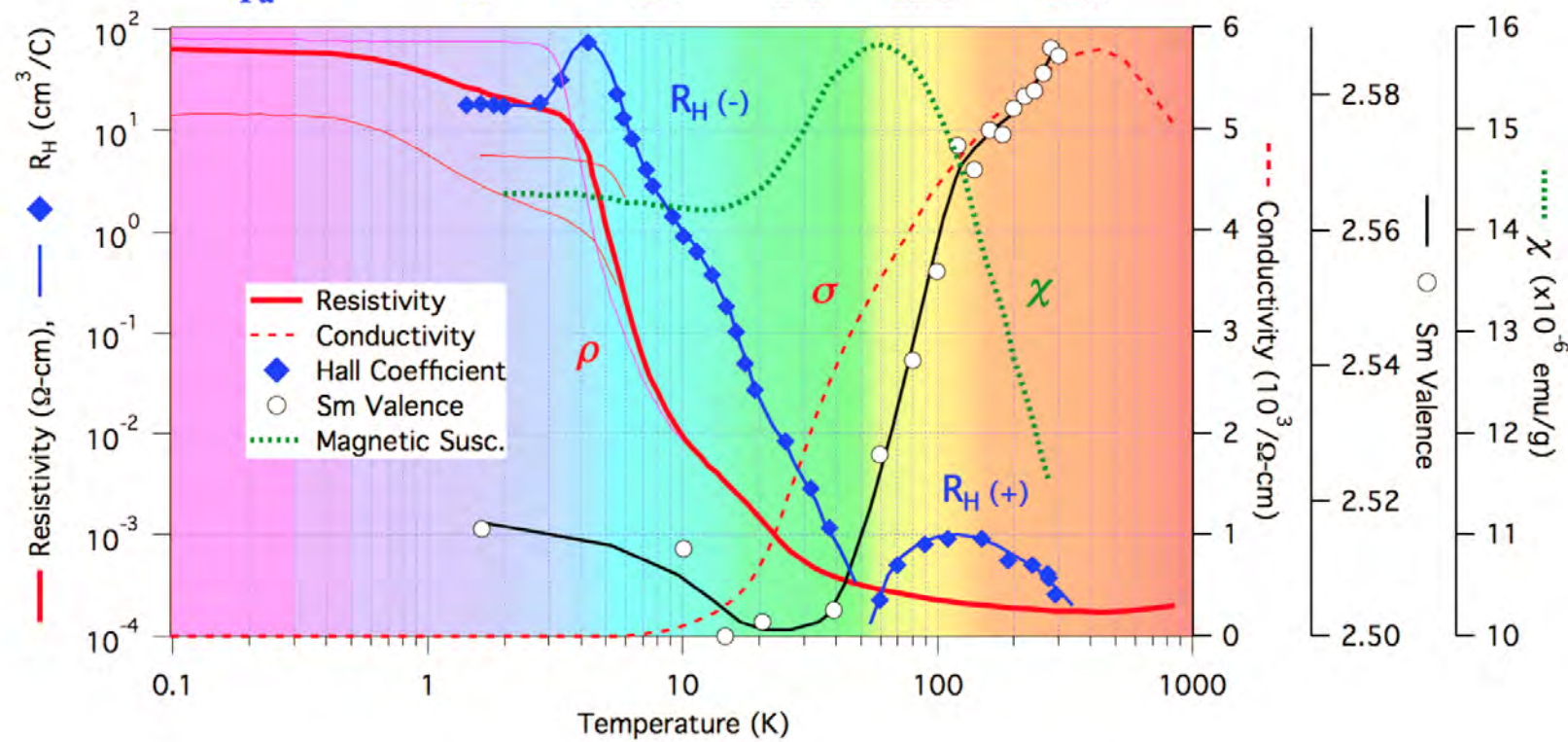


**Figure S1. Temperature regimes of the  $\text{SmB}_6$  transport and valence.** The three main transport regimes of  $\text{SmB}_6$  illustrated by comparison of resistivity/conductivity<sup>1</sup>, Hall coefficient<sup>2,3</sup> and bulk valence<sup>4</sup> and magnetic susceptibility<sup>5</sup>: (I) low temperature low carrier “in-gap state” regime below 4K, (II) intermediate metallic-to-insulating transition regime with negative Hall coefficient, and (III) high temperature poor-metal regime with positive Hall coefficient above 60K. Multiple low temperature resistivity profiles are plotted to illustrate the variation of the low temperature residual conduction found in the literature. A further subdivision of each regime into two sub-regimes is readily apparent from the various profiles.

# Topological Kondo Insulators

Maxim Dzero,<sup>1,2</sup> Jing Xia,<sup>3</sup> Victor Galitski,<sup>4,5</sup>  
and Piers Coleman<sup>6,7</sup>

Annu. Rev. Condens. Matter Phys. 2016. 7:249–80

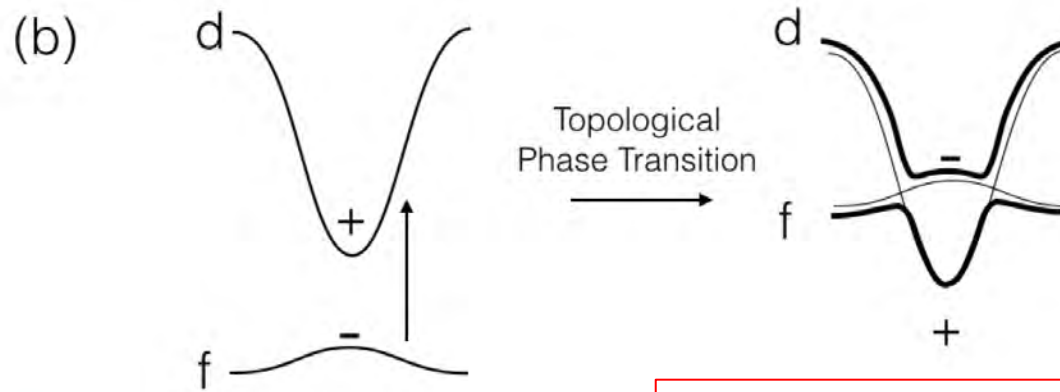


Figure 4

(a) If we ignore the effects of topology in a conventional metal and turn on interactions adiabatically. When the interactions are turned on, the bands split and the d-band becomes the upper band. Two bands of the same parity will always repel one-another and will not cross when

**4f-5d inversion:  
intermediate 4f valence**

Note:

SmB<sub>6</sub> mixed-valent: homogenous in space but inhomogenous in k-space  
Fe<sub>3</sub>O<sub>4</sub> mixed-valent: inhomogenous in space but homogenous in k-space

# Temperature dependence of the samarium oxidation state in $\text{SmB}_6$ and $\text{Sm}_{1-x}\text{La}_x\text{B}_6$

J. M. Tarascon, Y. Isikawa (\*), B. Chevalier, J. Etourneau, P. Hagenmuller  
and M. Kasaya

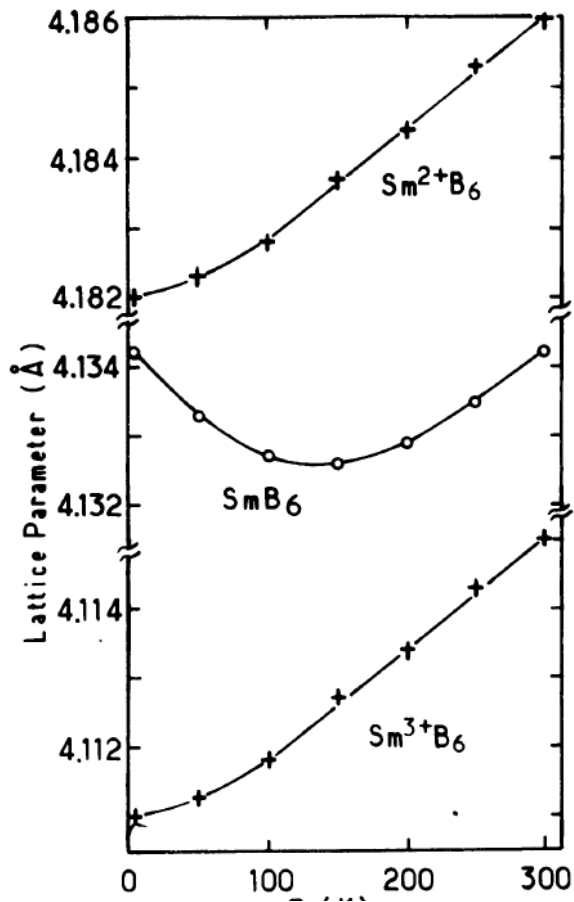


Fig. 1. — Lattice parameter temperature dependence of the cubic unit cell of  $\text{SmB}_6$  (experimental) and of the hypothetical hexaborides  $\text{Sm}^{2+}\text{B}_6$  and  $\text{Sm}^{3+}\text{B}_6$  (calculated).

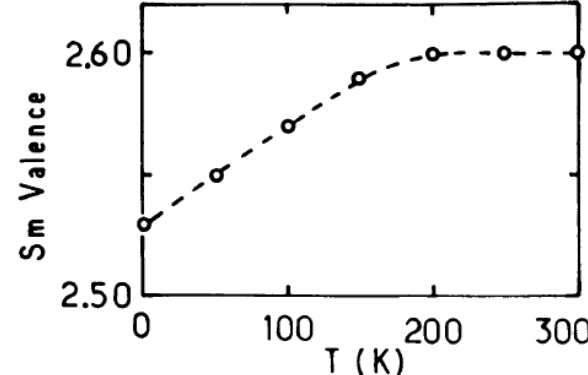
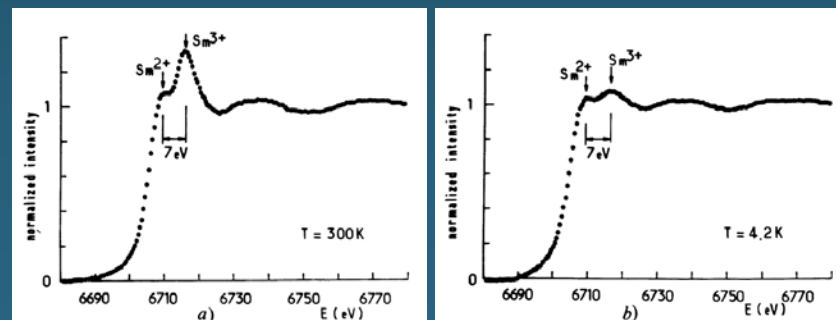
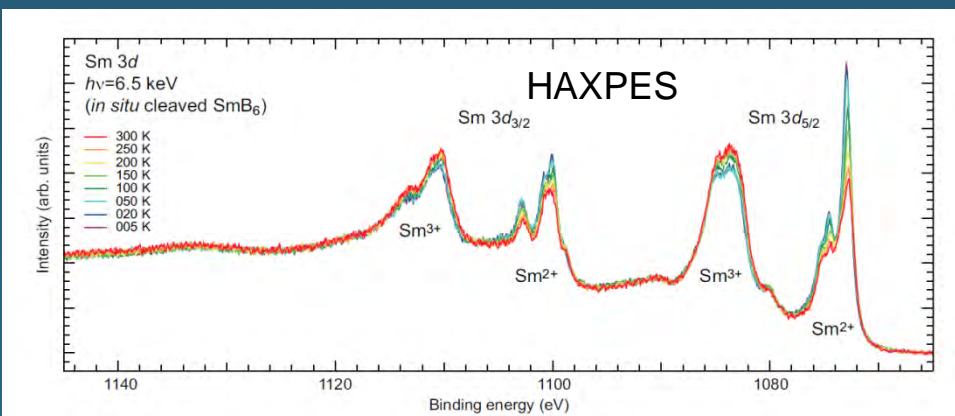
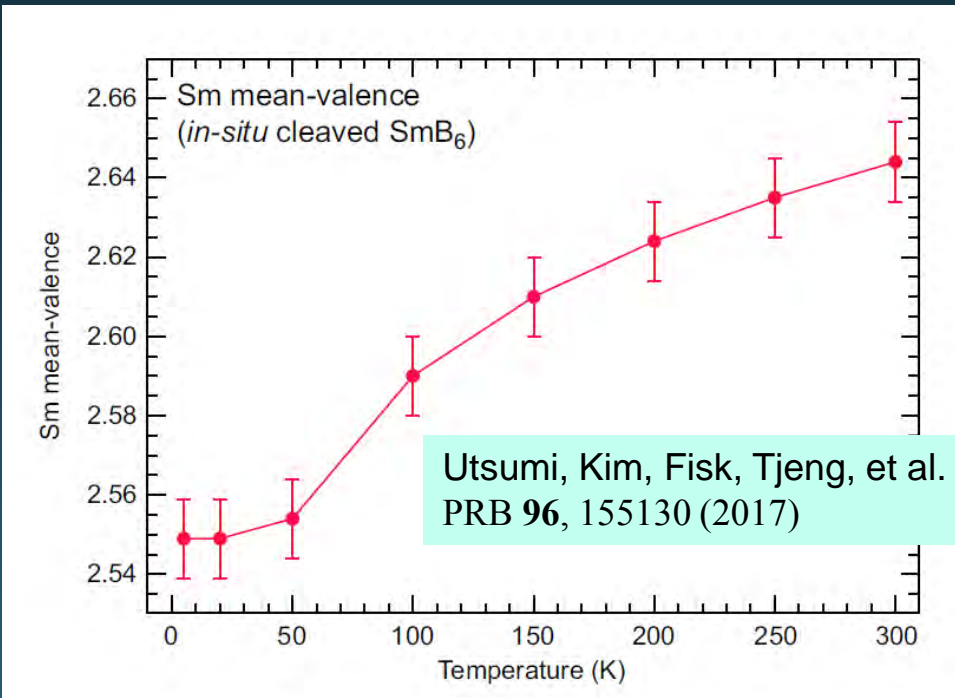


Fig. 3. — Average samarium valence temperature dependence in  $\text{SmB}_6$  between 300 K and 4.2 K.



# $\text{SmB}_6$ : an intermediate valence system

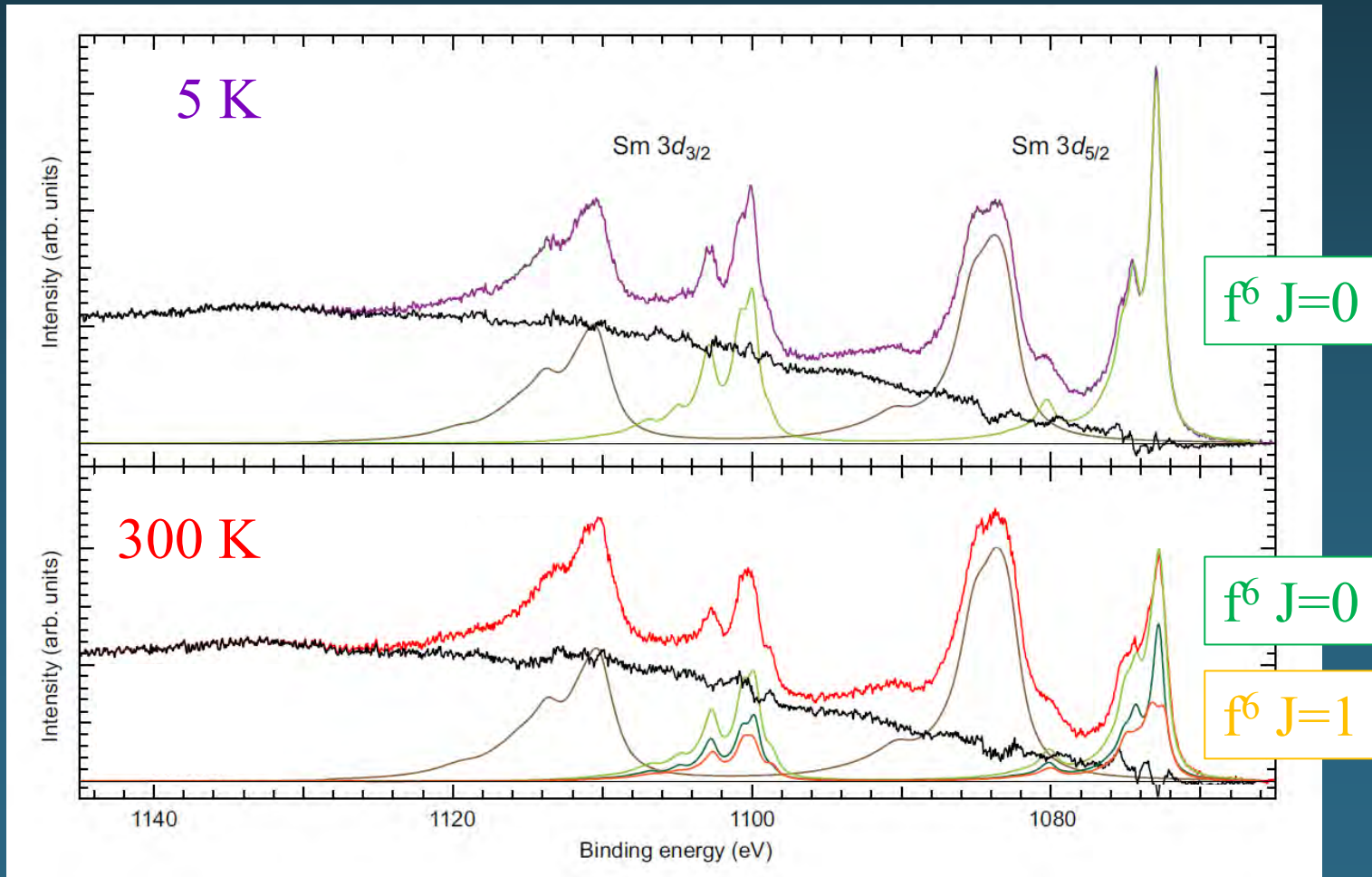


# $\text{SmB}_6$ : an intermediate valence system

PHYSICAL REVIEW B 96, 155130 (2017)

## Bulk and surface electronic properties of $\text{SmB}_6$ : A hard x-ray photoelectron spectroscopy study

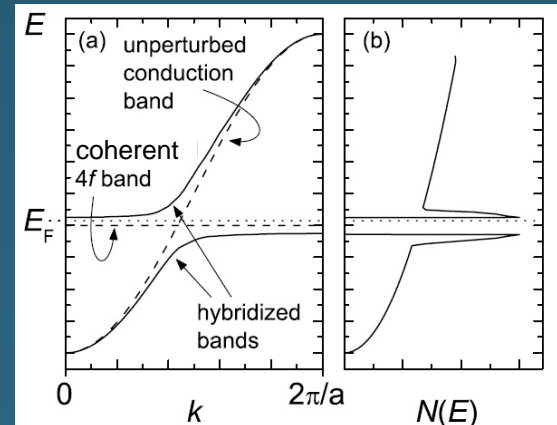
Y. Utsumi,<sup>1,\*</sup> D. Kasinathan,<sup>1</sup> K.-T. Ko,<sup>1</sup> S. Agrestini,<sup>1</sup> M. W. Haverkort,<sup>1,†</sup> S. Wirth,<sup>1</sup> Y.-H. Wu,<sup>2</sup> K.-D. Tsuei,<sup>2</sup> D.-J. Kim,<sup>3</sup> Z. Fisk,<sup>3</sup> A. Tanaka,<sup>4</sup> P. Thalmeier,<sup>1</sup> and L. H. Tjeng<sup>1</sup>



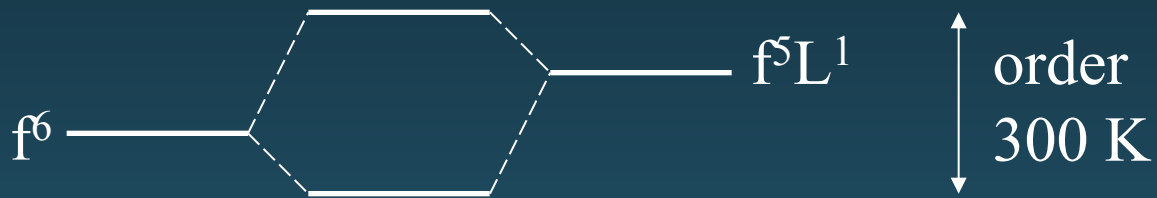
# What entropy drives the valence change in SmB<sub>6</sub> ?

- Lattice ??
  - lattice shrinks in going from 5 to 140 K
  - lattice expands from 140 K to 300 K, but valence still keeps increasing although there is more room for the bigger Sm<sup>2+</sup>
- Spin !!
  - Sm<sup>2+</sup> <sup>7</sup>F<sub>0</sub> (J=0, singlet) to Sm<sup>3+</sup> <sup>6</sup>H<sub>5/2</sub> (J=5/2, sextet)
- Similarities with Yb Kondo/heavy-fermion systems
  - Yb valence increases from low T to high T, e.g. Yb<sup>2.8+</sup> to Yb<sup>2.9+</sup>
  - YbInCu<sub>4</sub>: sudden expansion of lattice upon cooling !!

Sm<sup>2+</sup> f<sup>6</sup> J=0: even number of electrons  
→ hybridization gap model



## How to set up the energy level diagram of $\text{SmB}_6$ ??

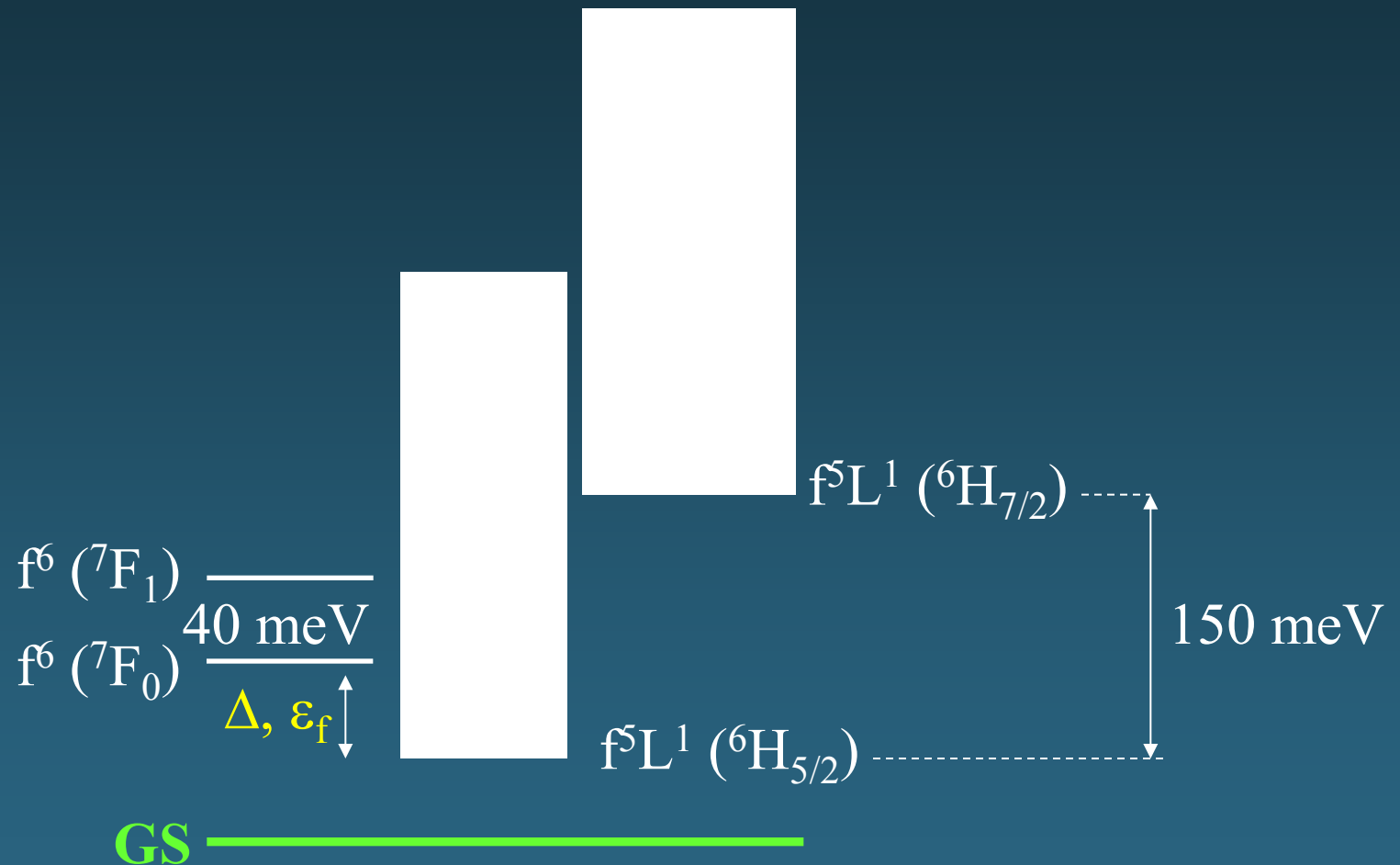


energy separation much smaller than hopping integral  
(to get valence close to 2.5+)

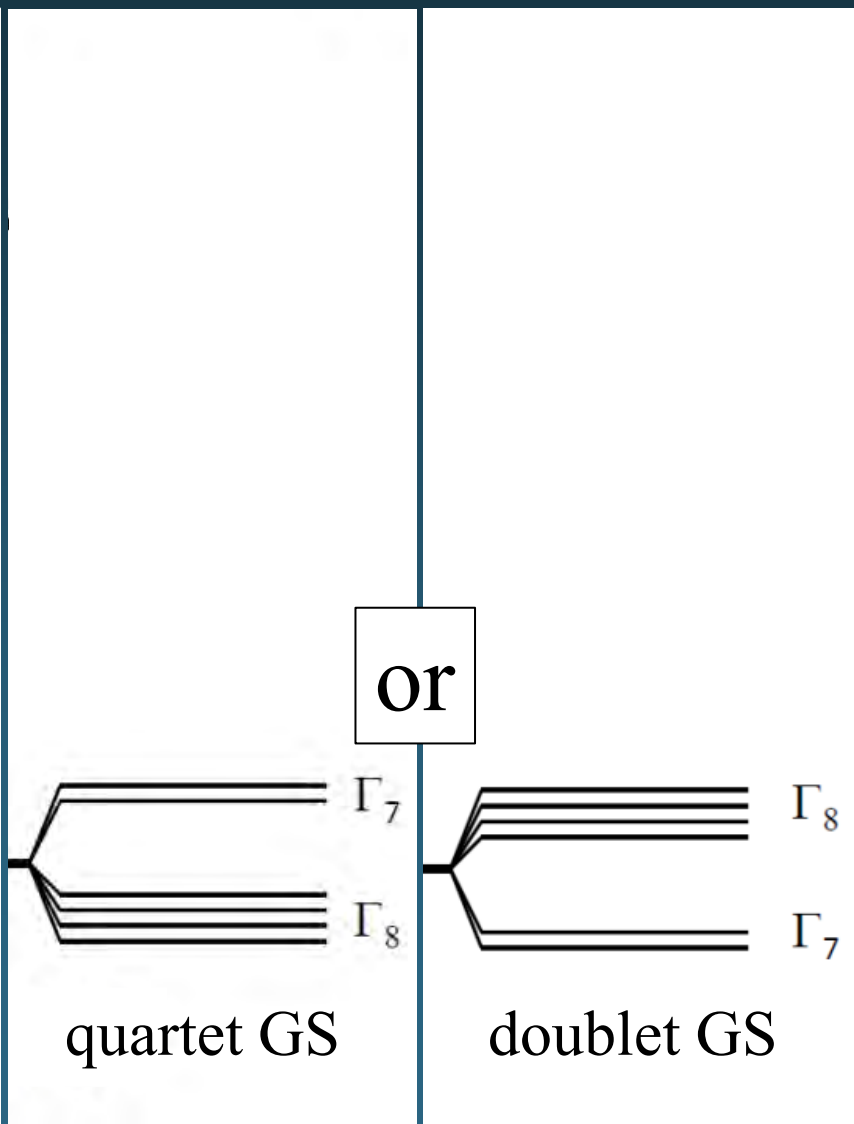
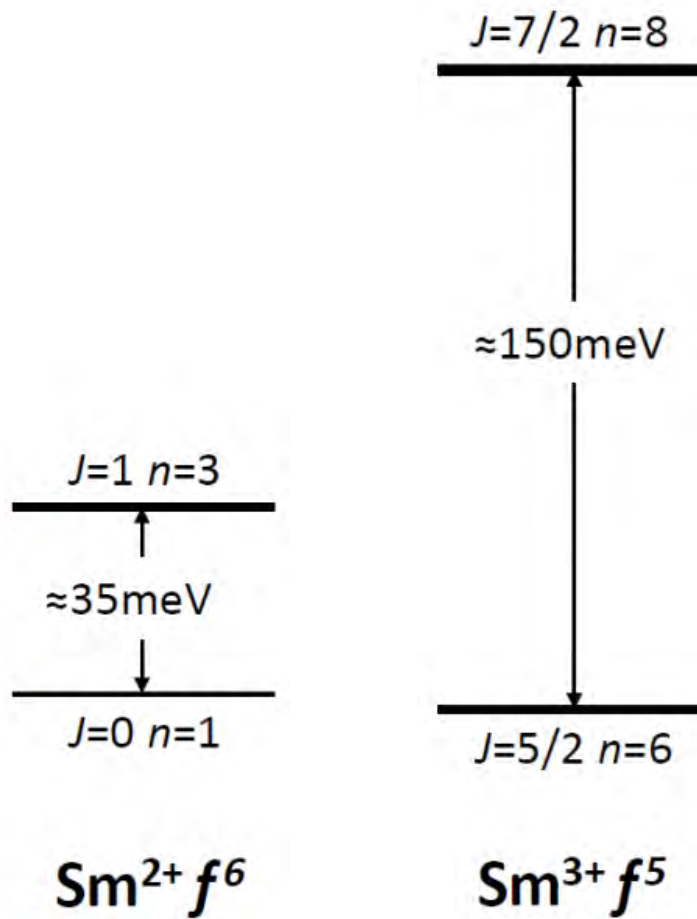
### Problems:

- from low T to high T: valence move always towards 2.5+
- lattice expansion with T tends to lower the  $\text{f}^6$  energy

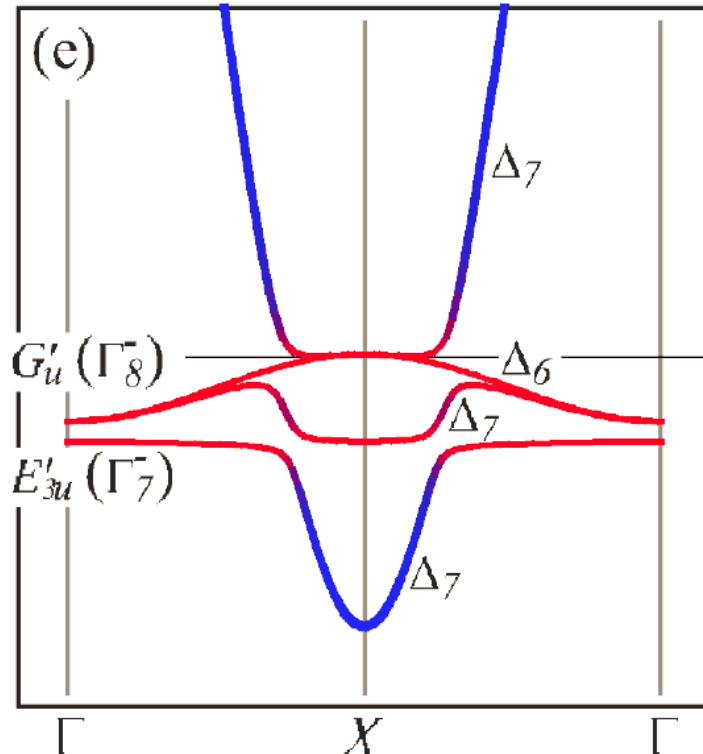
# How to set up the energy level diagram of SmB<sub>6</sub> ??



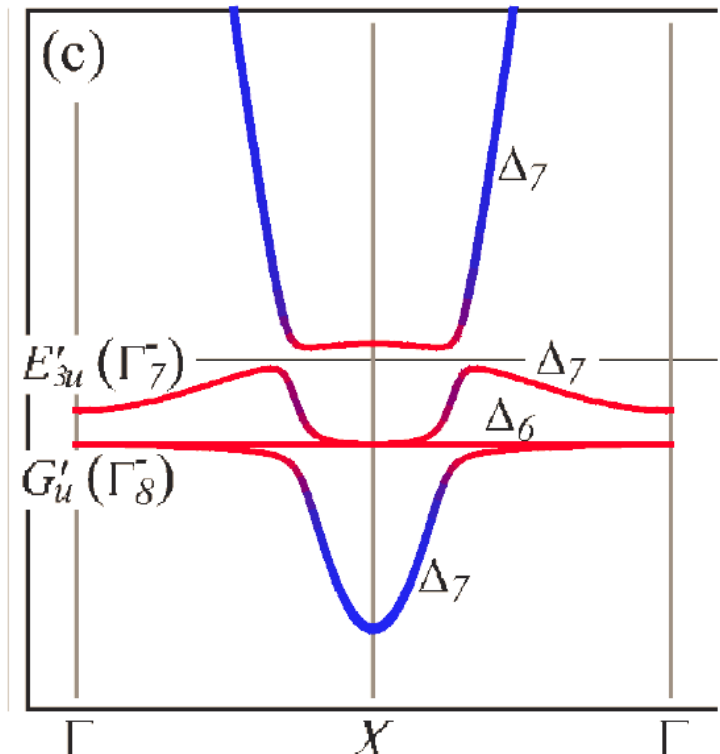
# Energy level diagram in intermediate valent SmB<sub>6</sub>



quartet GS



doublet GS



hybridization gap \*may\* open

hybridization gap \*will\* open

?? Ground state of the Sm 4f<sup>5</sup> configuration of SmB<sub>6</sub>:  $\Gamma_7$  or  $\Gamma_8$  ??

## Consequences: spin-texture of topological surface states

PRL 115, 156405 (2015)

PHYSICAL REVIEW LETTERS

week ending  
9 OCTOBER 2015

### Surface-State Spin Textures and Mirror Chern Numbers in Topological Kondo Insulators

Markus Legner, Andreas Rüegg, and Manfred Sigrist

PRL 115, 156404 (2015)

PHYSICAL REVIEW LETTERS

week ending  
9 OCTOBER 2015

### Distinct Topological Crystalline Phases in Models for the Strongly Correlated Topological Insulator SmB<sub>6</sub>

Pier Paolo Baruselli and Matthias Vojta

PHYSICAL REVIEW B 93, 195117 (2016)

### Spin textures on general surfaces of the correlated topological insulator SmB<sub>6</sub>

Pier Paolo Baruselli and Matthias Vojta

# Consequences: spin-texture of topological surface states

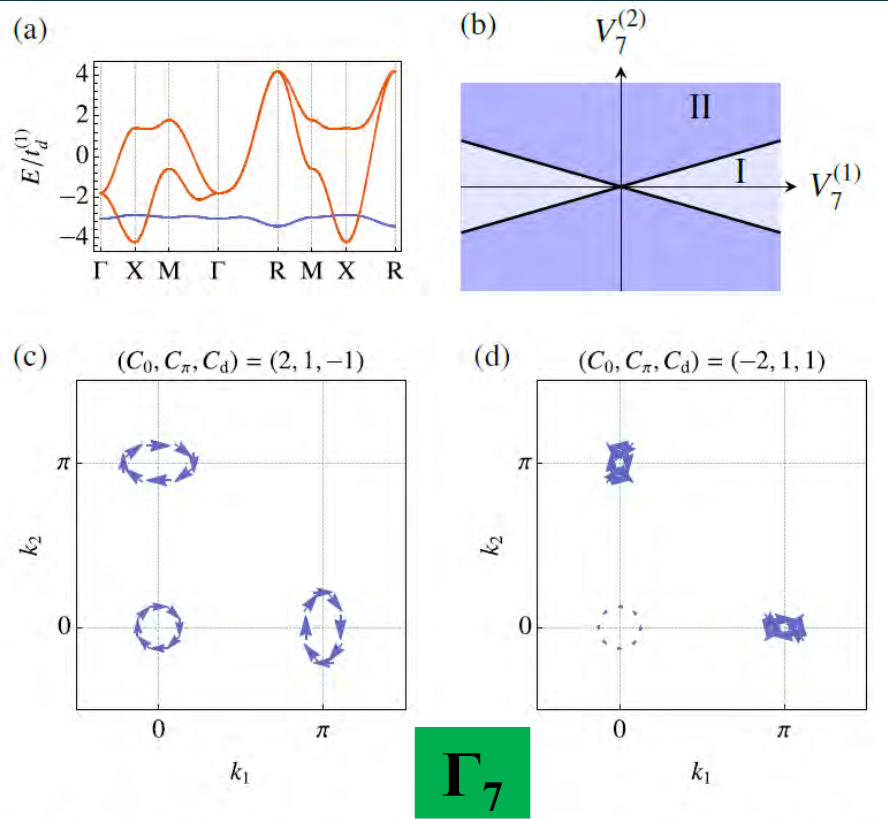


FIG. S2. Bandstructure without hybridization (a) and phase diagram (b) for the  $\Gamma_7$  model defined in Eq. (S10) and (S8) with  $t_d^{(1)} = 1$ ,  $t_d^{(2)} = -0.2$ ,  $t_7^{(1)} = -0.03$ ,  $t_7^{(2)} = 0.02$ , and  $\epsilon_7 = -3$ . The two different spin textures (c-d) in phases I and II, respectively, are shown for hybridization parameters  $(V_7^{(1)}, V_7^{(2)}) = (0.3, 0)$  and  $(V_7^{(1)}, V_7^{(2)}) = (0.1, 0.1)$ , respectively. Due to the negative eigenvalue of the restricted spin operator for  $f$  electrons (Eq. (14)), the spin direction is reversed around all HSPs when compared to Fig. 1. Note that the

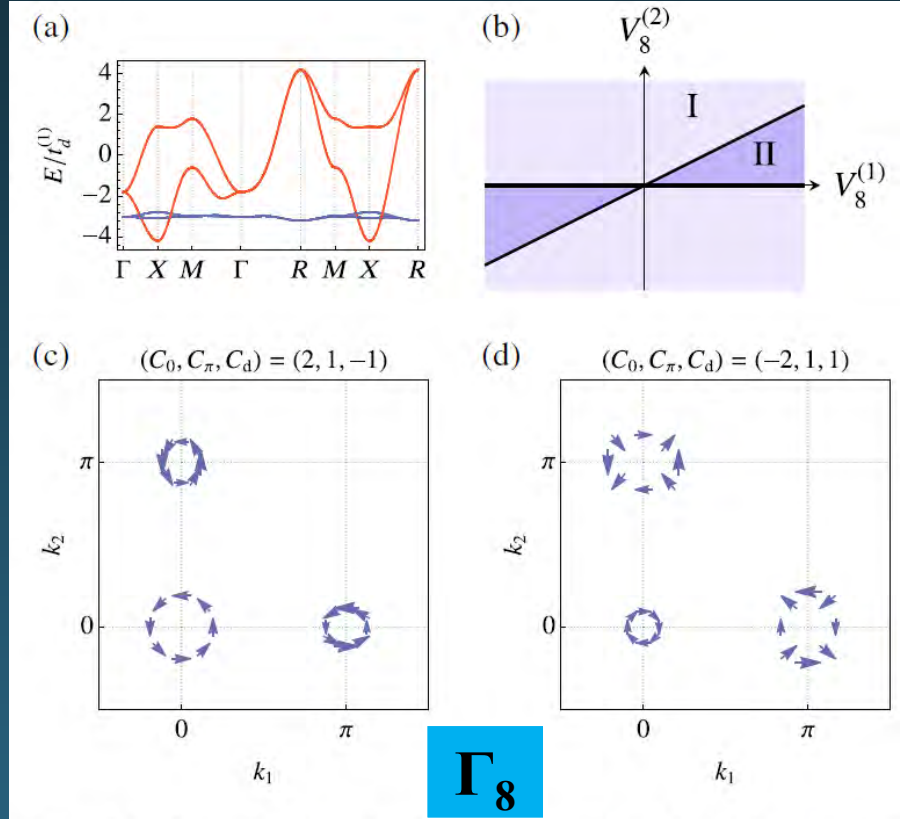
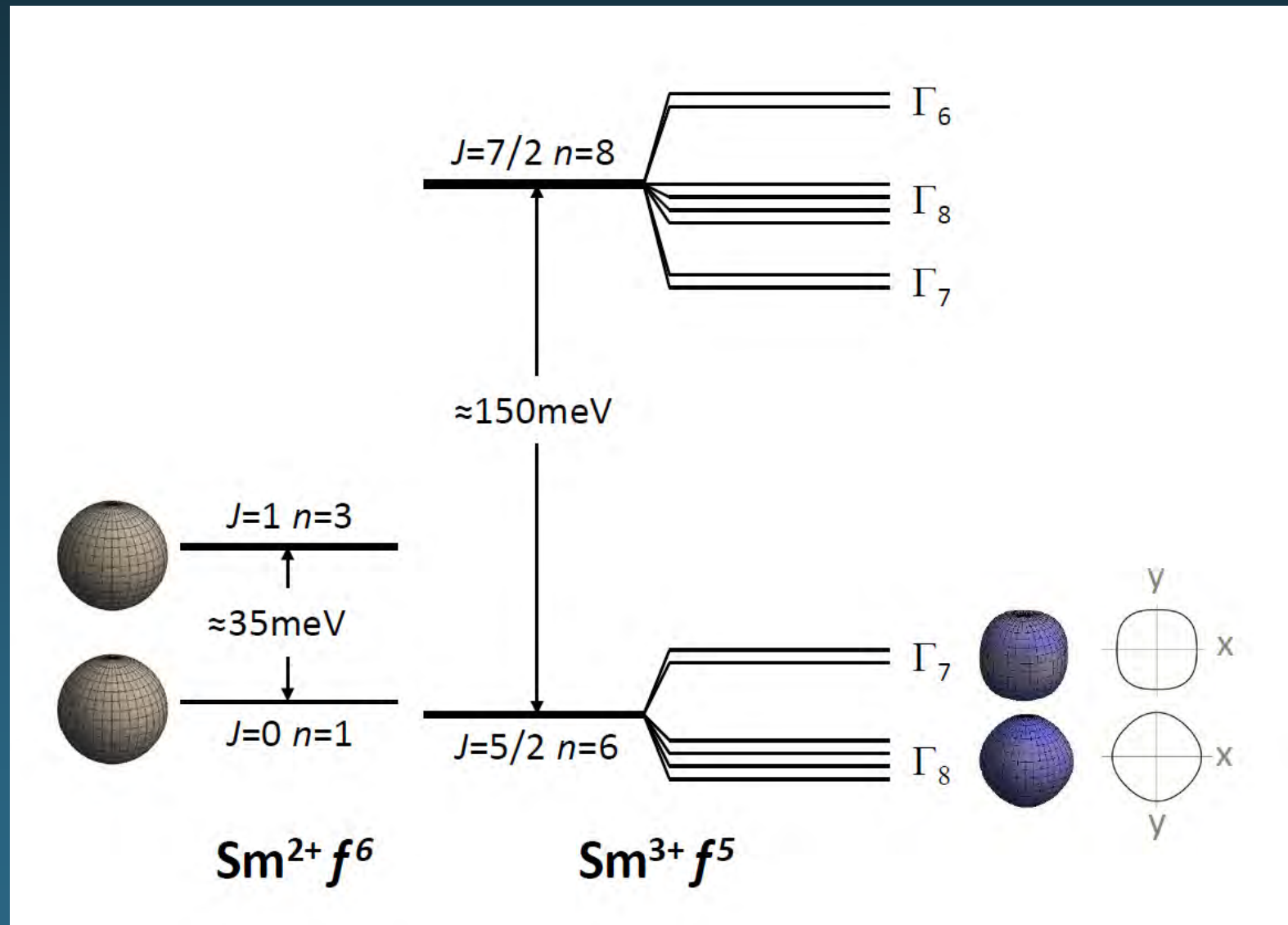
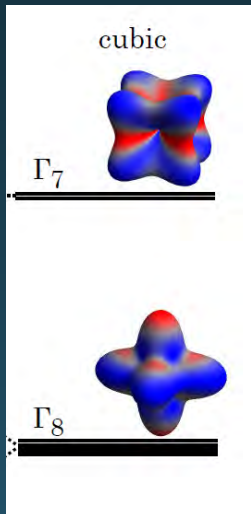


FIG. 3 (color online). Band structure without hybridization (a) and phase diagram (b) for the  $\Gamma_8$  model defined in Eq. (9) with  $t_d^{(1)} = 1$ ,  $t_d^{(2)} = -0.2$ ,  $t_8^{(1)} = -0.03$ ,  $t_8^{(2)} = 0.02$ , and  $\epsilon_8 = -3$ . The two spin textures [(c),(d)] in phases I and II, respectively, are realized for the hybridization parameters  $(V_8^{(1)}, V_8^{(2)}) = (0.3, 0.07)$  and  $(V_8^{(1)}, V_8^{(2)}) = (-0.1, 0.1)$ , respectively.

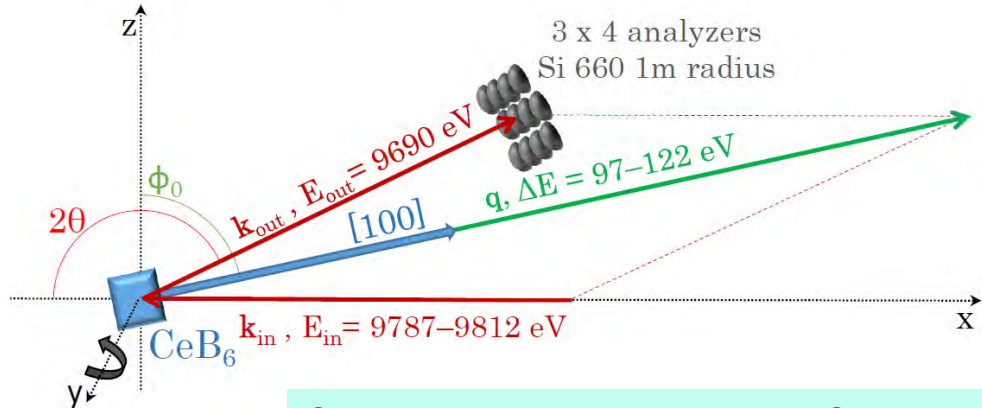
# Can core level NIXS solve the SmB<sub>6</sub> symmetry problem ??



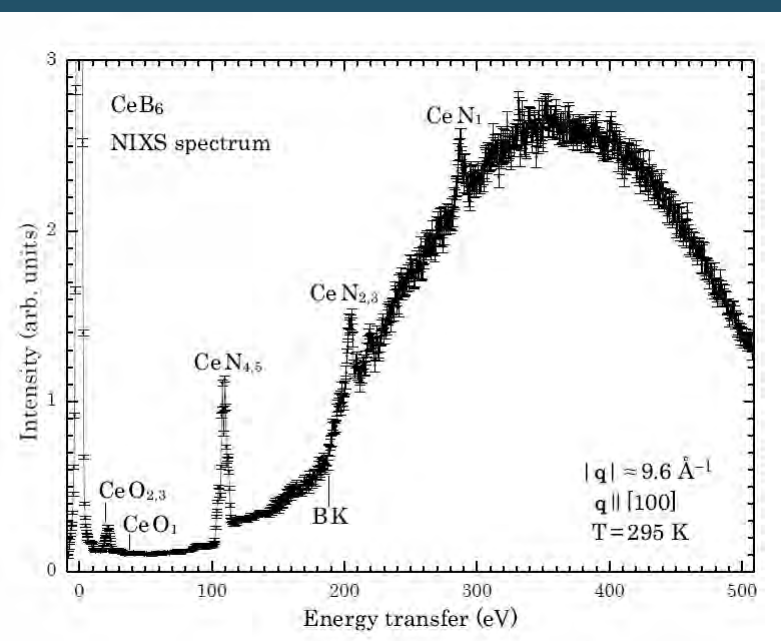
# The quartet ground state of CeB<sub>6</sub>



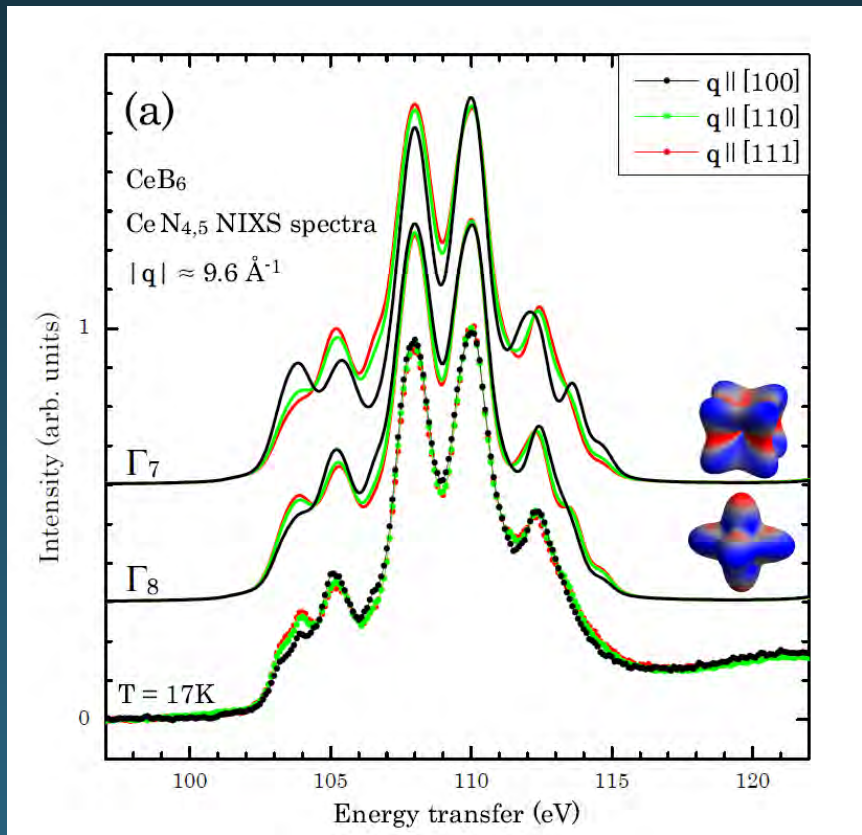
Inelastic X-ray Scattering geometry



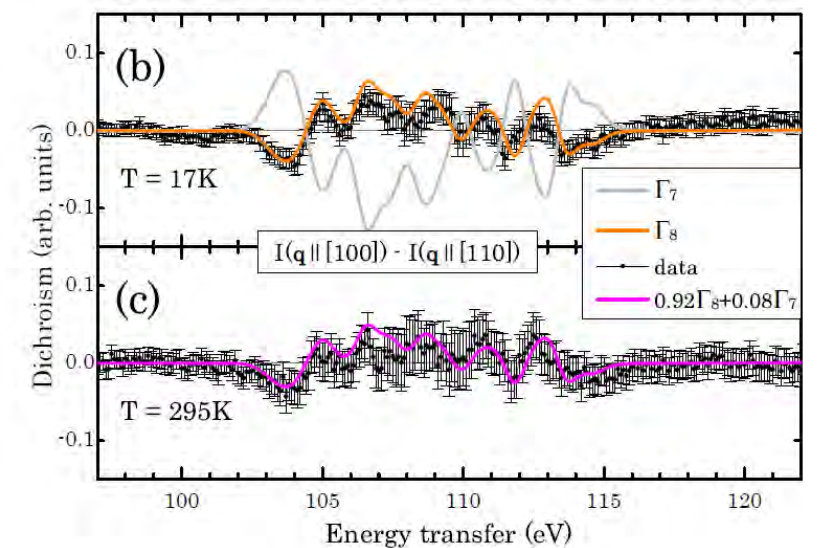
Sundermann, Lee, Fisk, Tjeng, Severing et al.  
EPL, **117** (2017) 17003



# The quartet ground state of CeB<sub>6</sub>



Sundermann, Lee, Fisk, Tjeng, Severing et al.  
EPL, 117 (2017) 17003



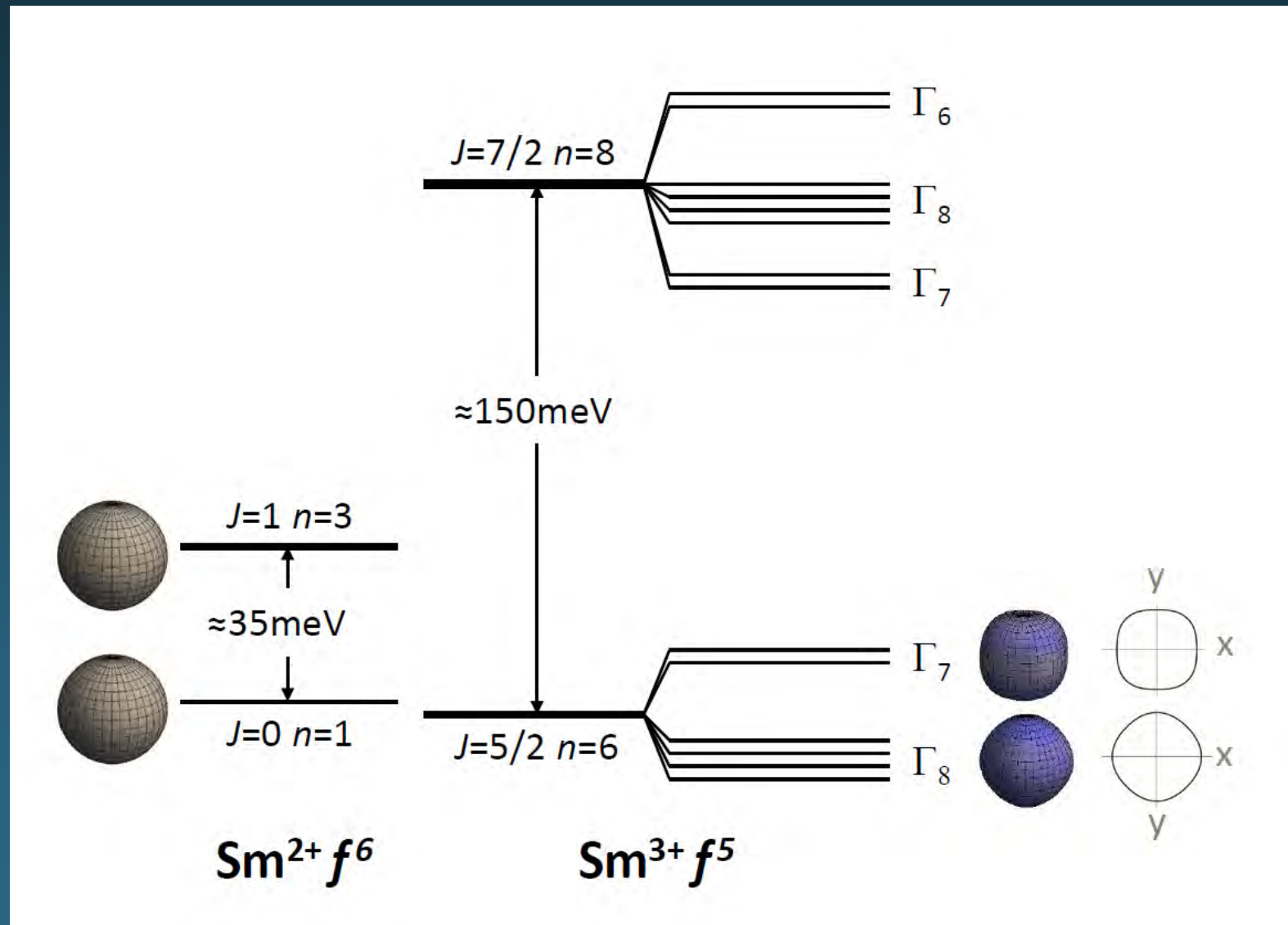
## The quartet ground state in CeB<sub>6</sub>: An inelastic x-ray scattering study

M. SUNDERMANN<sup>1,2</sup>, K. CHEN<sup>1</sup>, H. YAVAŞ<sup>3</sup>, HANOH LEE<sup>4</sup>, Z. FISK<sup>5</sup>, M. W. HAVERKORT<sup>2,6</sup>, L. H. TJENG<sup>2</sup> and A. SEVERING<sup>1,2</sup>

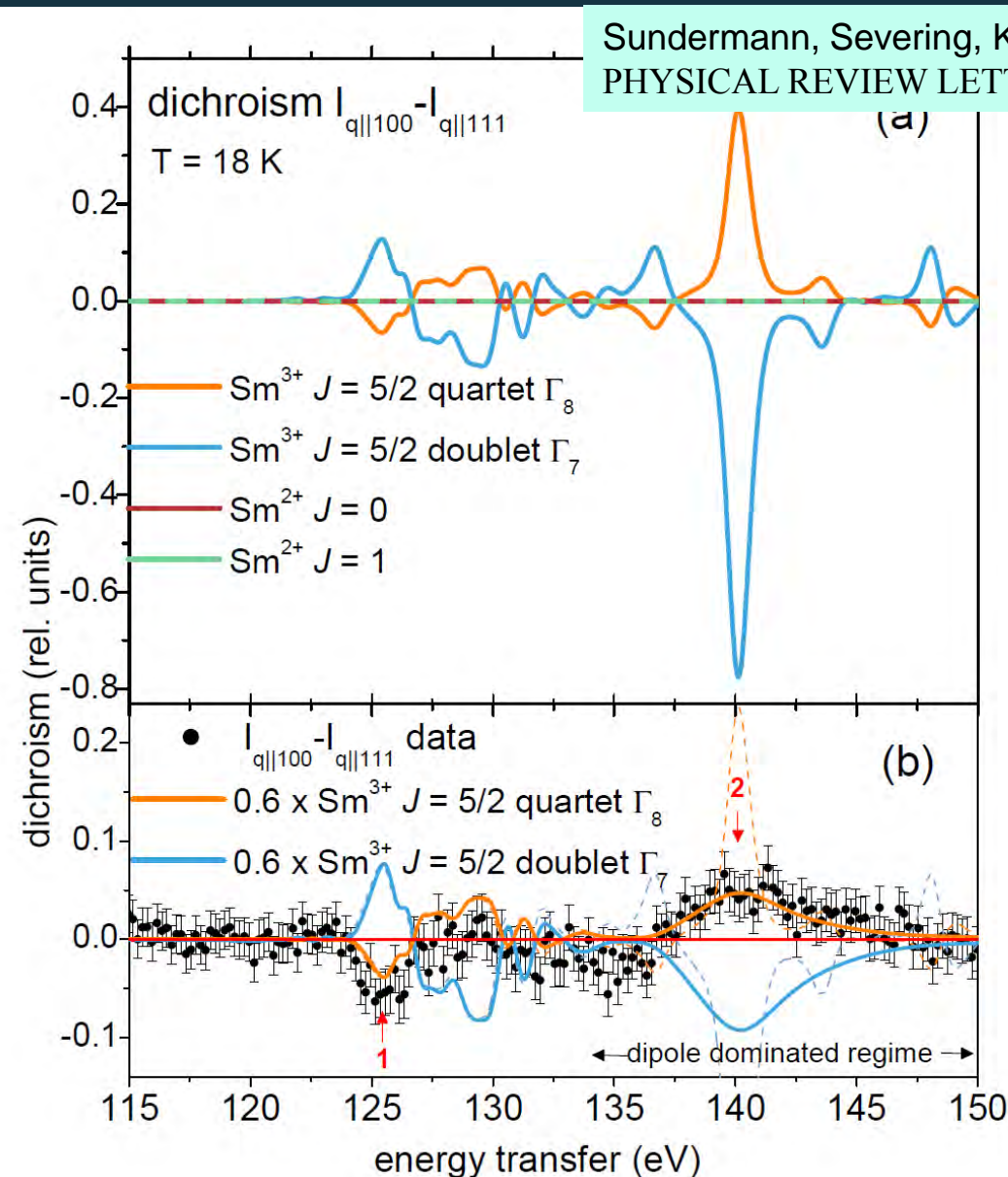
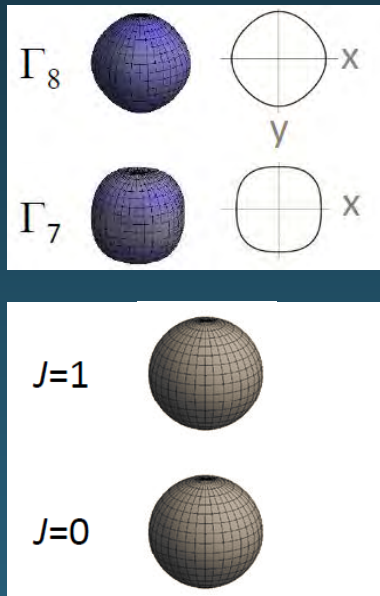
EPL, 117 (2017) 17003



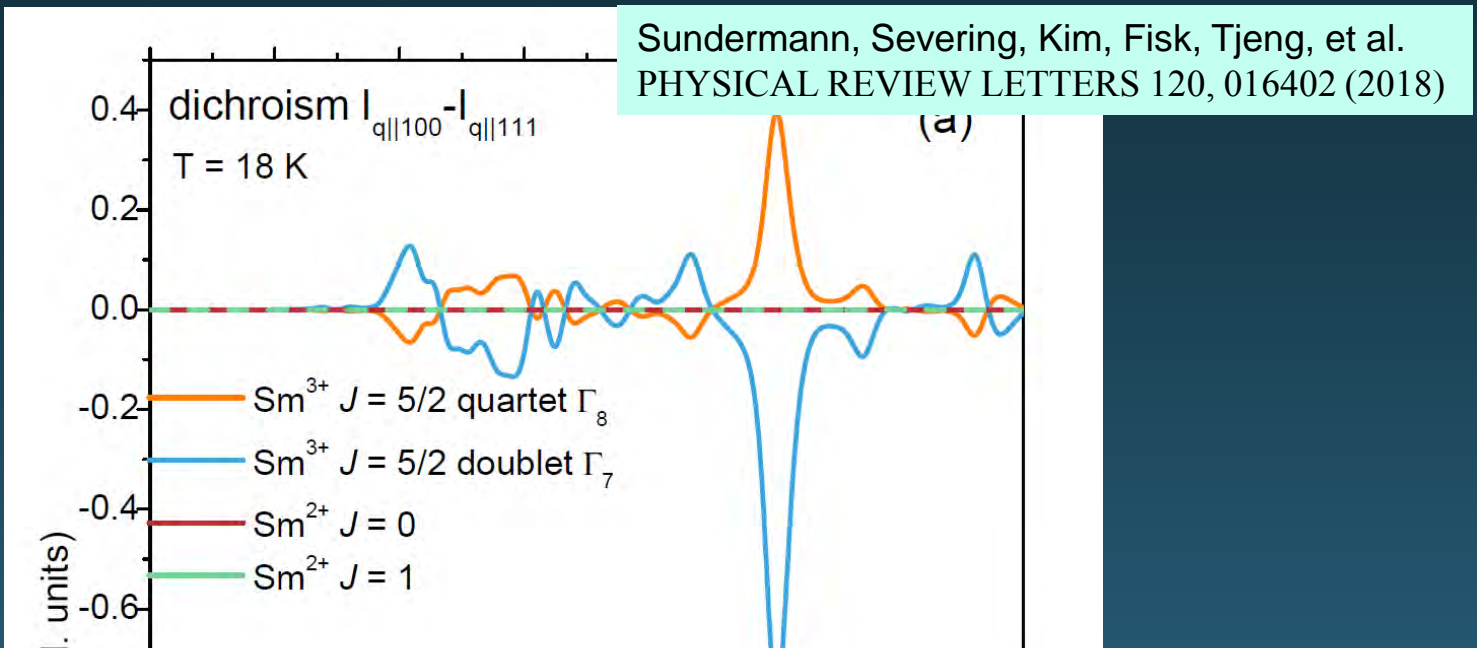
# Core level NIXS on SmB<sub>6</sub>



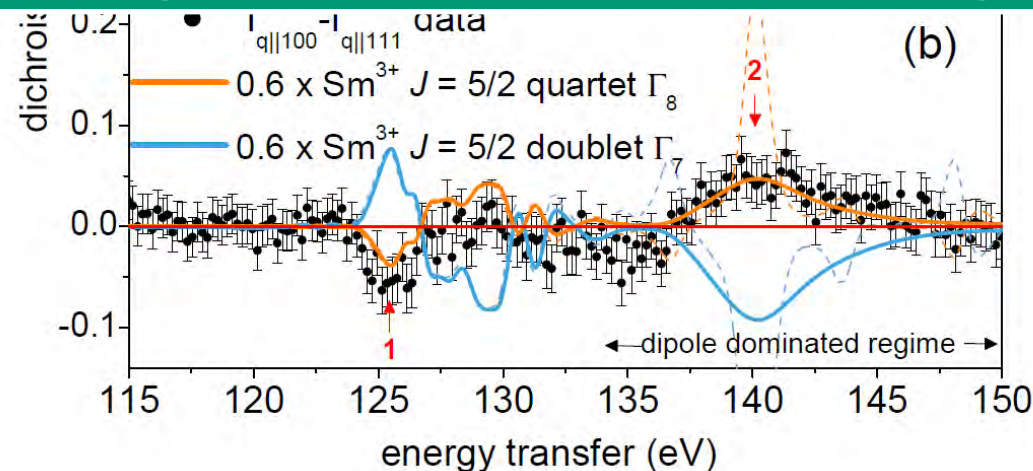
# Core level NIXS on $\text{SmB}_6$



# Core level NIXS on SmB<sub>6</sub>

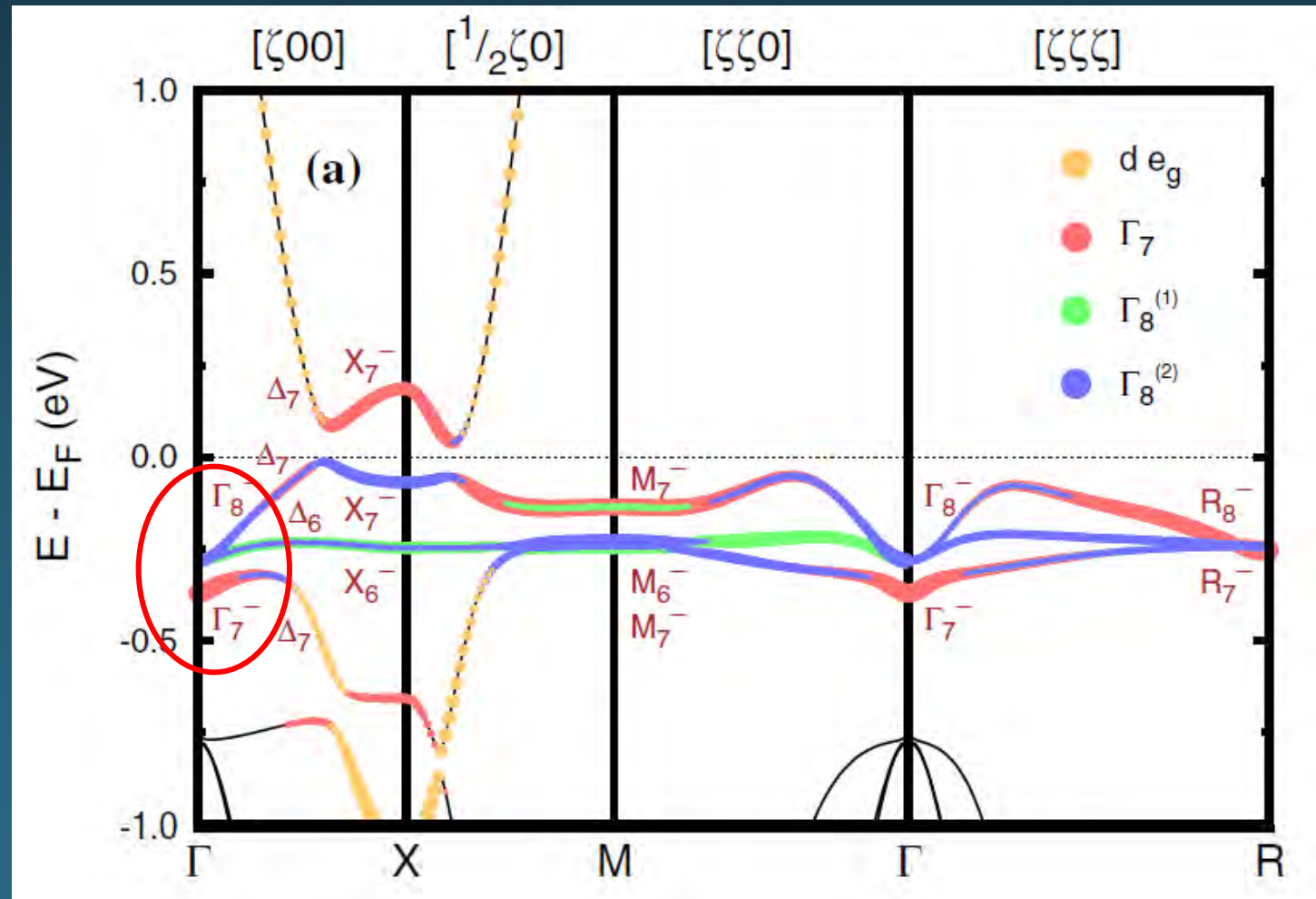


The  $\Gamma_8$  forms the ground state of the Sm 4f<sup>5</sup> configuration of SmB<sub>6</sub>



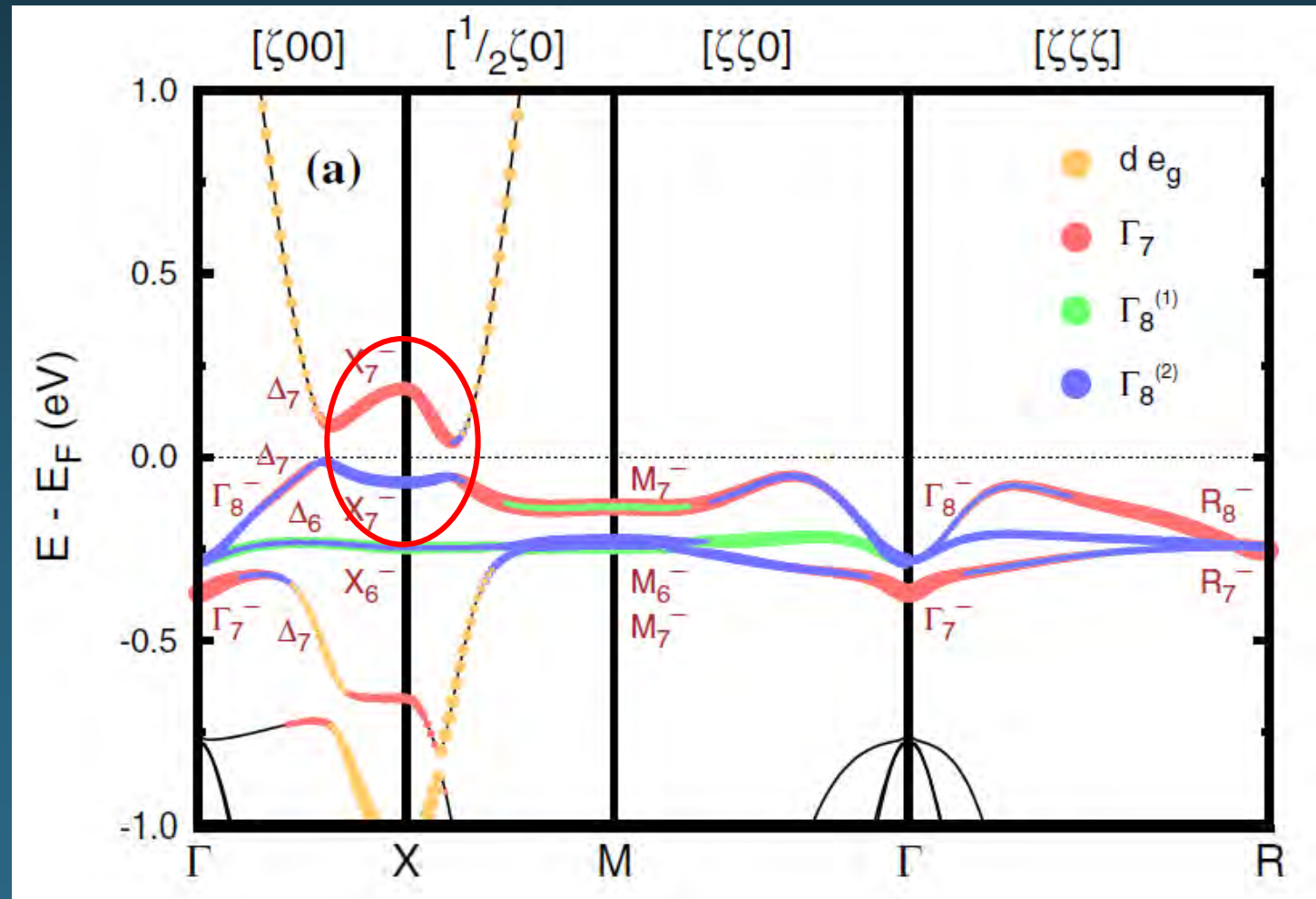
# Band Symmetries of Mixed-Valence Topological Insulator: SmB<sub>6</sub>

Chang-Jong Kang<sup>1</sup>, Junwon Kim<sup>1</sup>, Kyoo Kim<sup>1</sup>, Jeongsoo Kang<sup>2</sup>,  
Jonathan D. Denlinger<sup>3</sup>, and Byung Il Min<sup>1\*</sup>



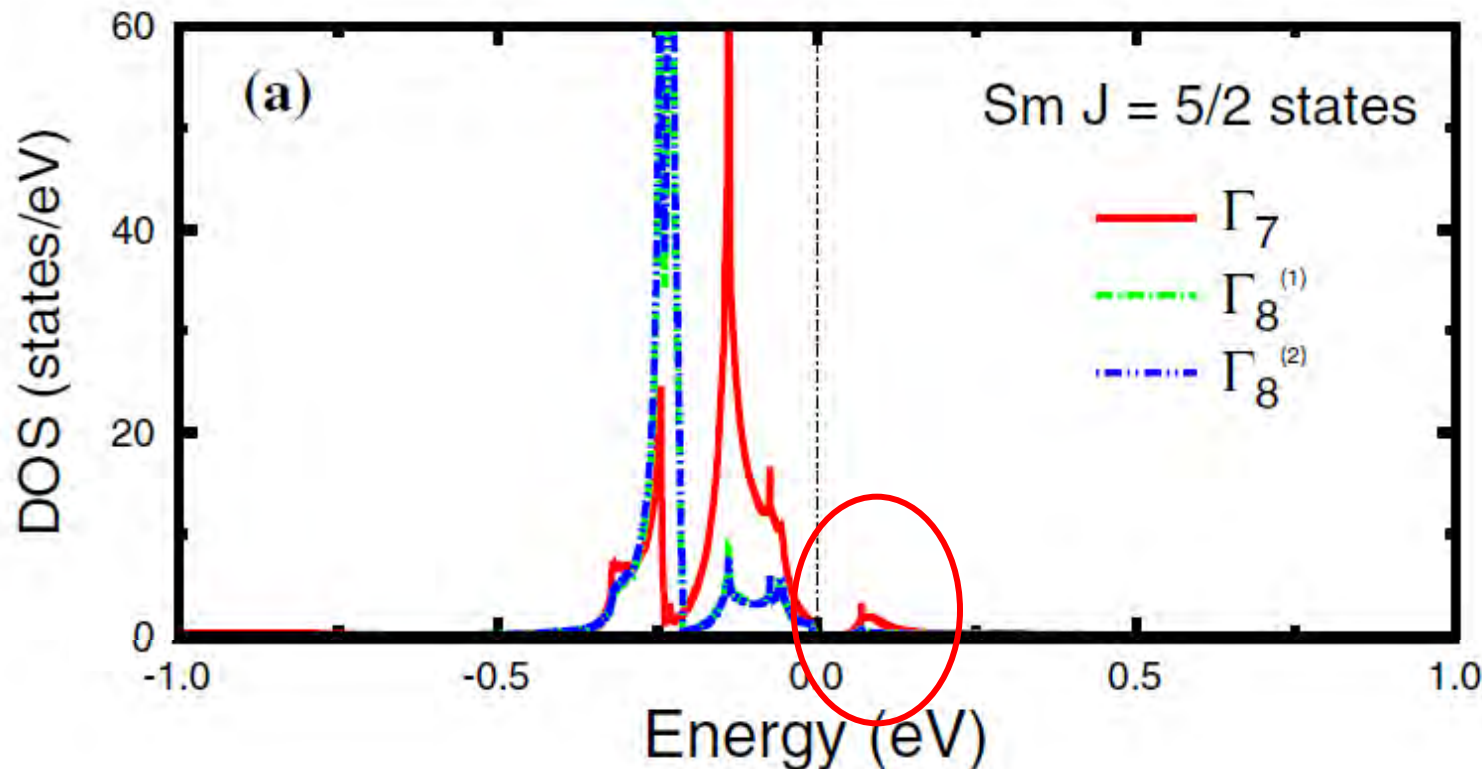
# Band Symmetries of Mixed-Valence Topological Insulator: SmB<sub>6</sub>

Chang-Jong Kang<sup>1</sup>, Junwon Kim<sup>1</sup>, Kyoo Kim<sup>1</sup>, Jeongsoo Kang<sup>2</sup>,  
Jonathan D. Denlinger<sup>3</sup>, and Byung Il Min<sup>1\*</sup>



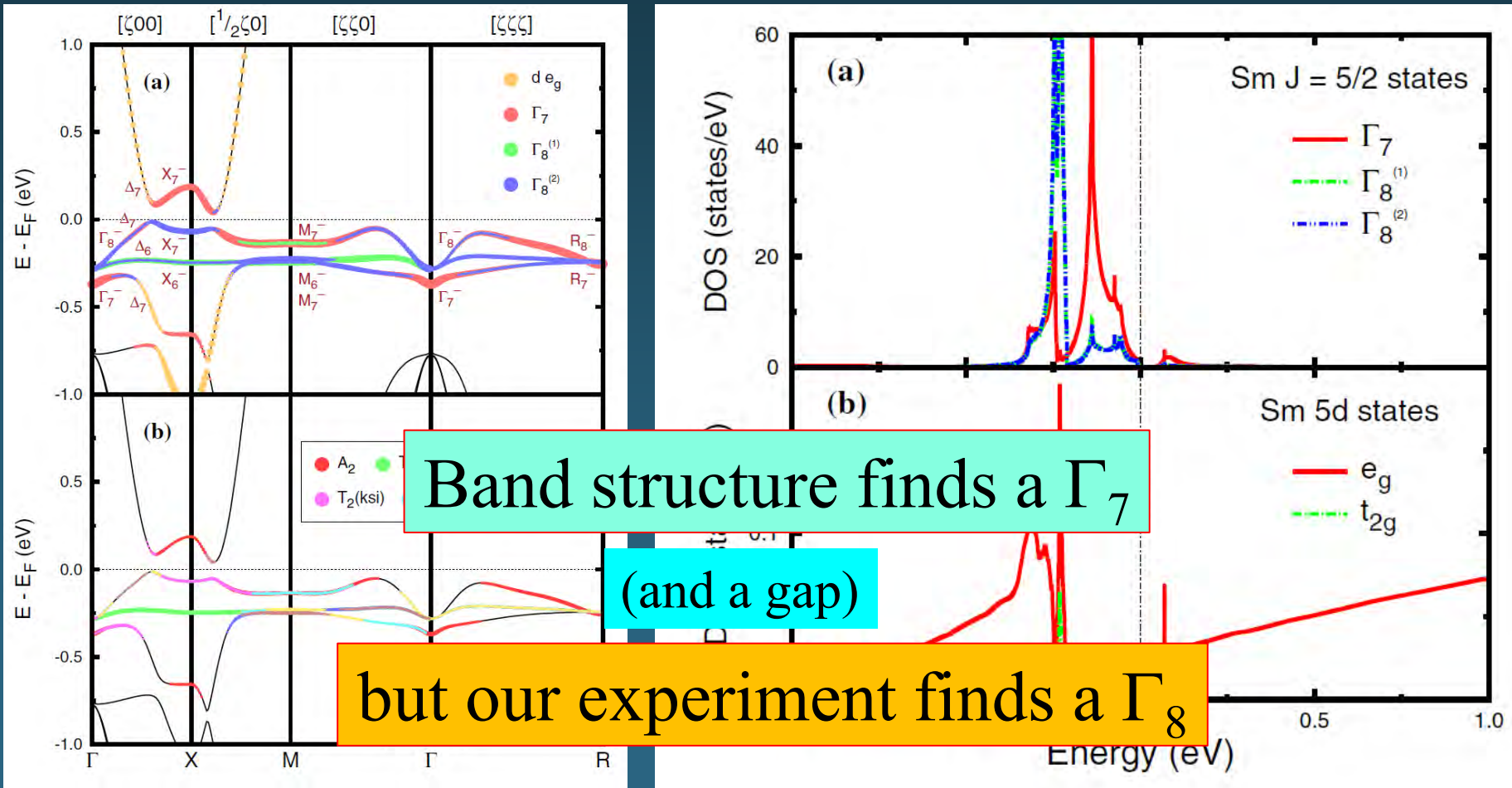
# Band Symmetries of Mixed-Valence Topological Insulator: SmB<sub>6</sub>

Chang-Jong Kang<sup>1</sup>, Junwon Kim<sup>1</sup>, Kyoo Kim<sup>1</sup>, Jeongsoo Kang<sup>2</sup>,  
Jonathan D. Denlinger<sup>3</sup>, and Byung Il Min<sup>1\*</sup>

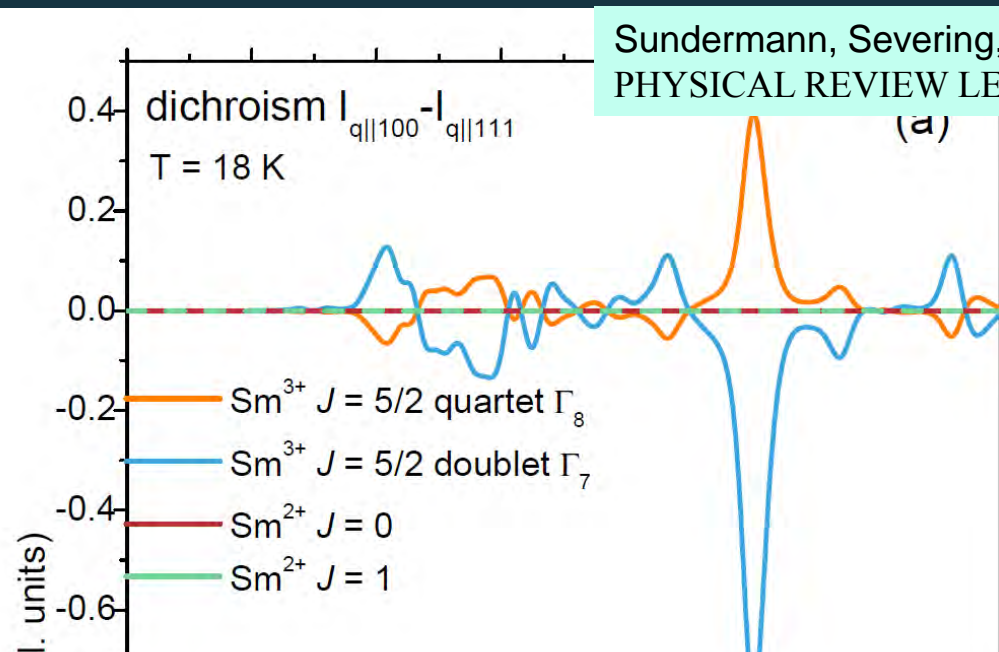
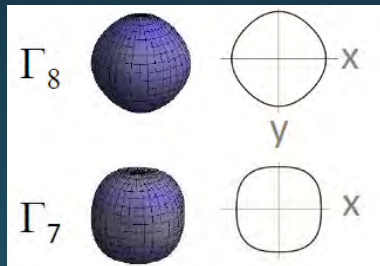


# Band Symmetries of Mixed-Valence Topological Insulator: SmB<sub>6</sub>

Chang-Jong Kang<sup>1</sup>, Junwon Kim<sup>1</sup>, Kyoo Kim<sup>1</sup>, Jeongsoo Kang<sup>2</sup>,  
 Jonathan D. Denlinger<sup>3</sup>, and Byung Il Min<sup>1\*</sup>



# Core level NIXS on $\text{SmB}_6$

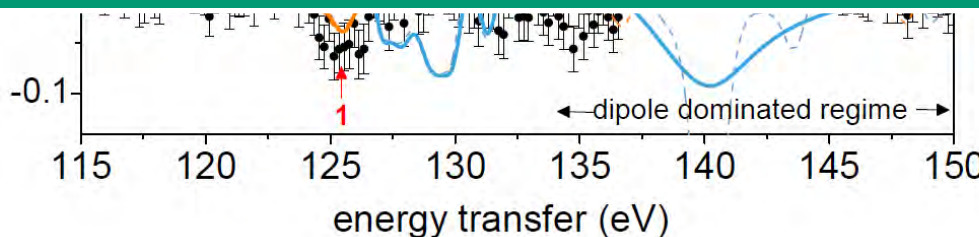


Full  $\Gamma_8$  polarization for the Sm 4f<sup>5</sup> configuration

→ Hardly any mixing in of the  $\Gamma_7$

→ Extremely narrow 4f bands

→ Low energy properties of  $\text{SmB}_6$  are built up from  $\Gamma_8$  states

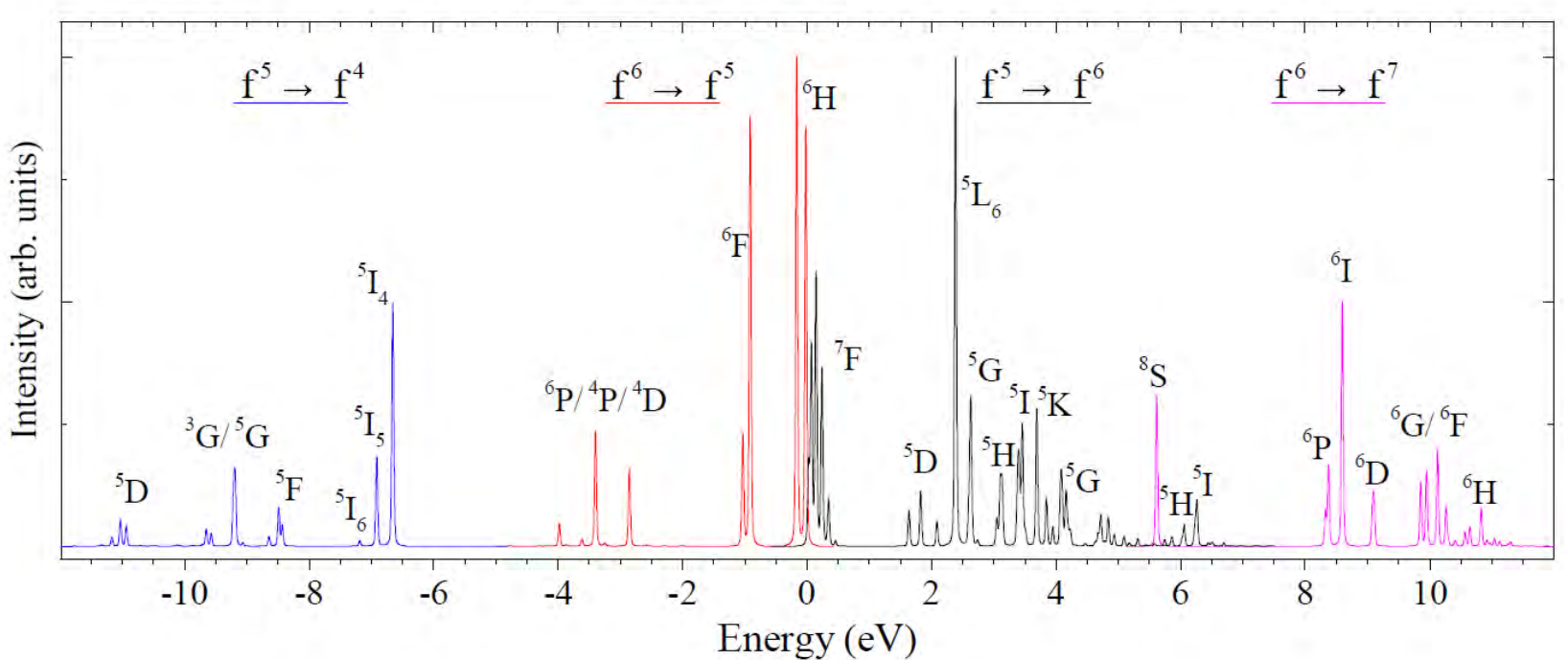


# Fractional Parentage

G.A. Sawatzky and R. Green

Lecture Notes of the Autumn School © ISBN 978-3-95806-159-0  
Correlated Electrons 2016

Eva Pavarini, Erik Koch, Jeroen van den Brink, and George Sawatzky (Eds.)



$f^6 (J=0, {}^7F_0) \rightarrow f^5 (\dots)$

small weight to  $f^5 (J=5/2, {}^6H_{5/2})$

$f^5 (J=5/2, {}^6H_{5/2}) \rightarrow f^6 (\dots)$

small weight to  $f^6 (J=0, {}^7F_0)$

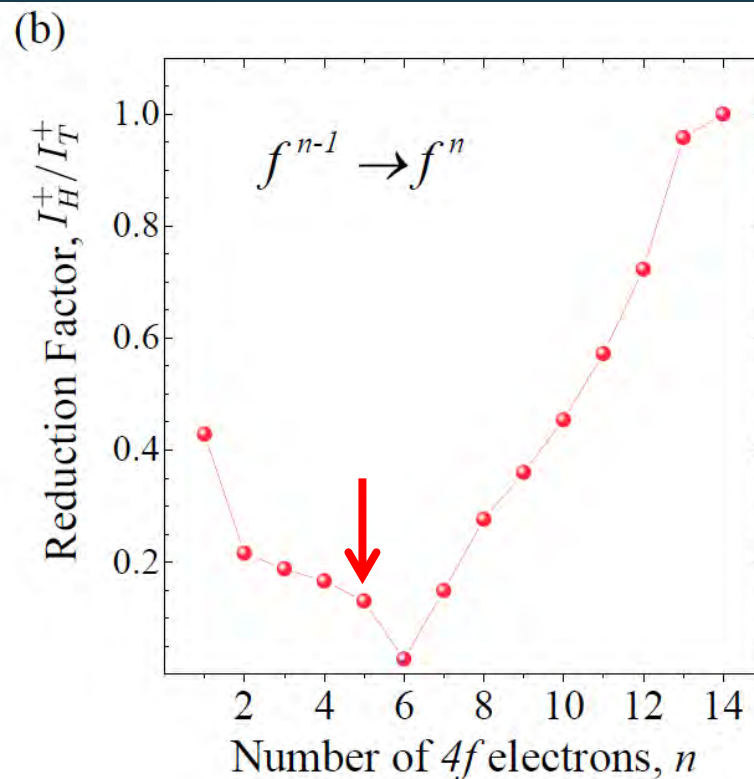
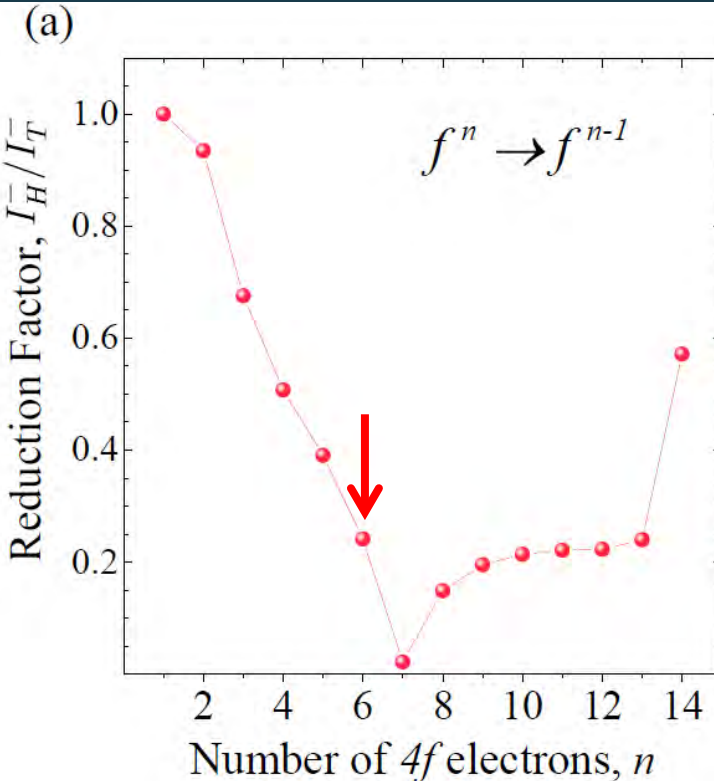
4f band formation:  $f^6(A, J=0) + f^5(B, J=5/2) \leftrightarrow f^5(A, J=5/2) + f^6(B, J=0)$

# Fractional Parentage

G.A. Sawatzky and R. Green

Lecture Notes of the Autumn School on  
Correlated Electrons 2016

Eva Pavarini, Erik Koch, Jeroen van den Brink, and George Sawatzky (Eds.)



4f band formation:  $f^6(A, J=0) + f^5(B, J=5/2) \leftrightarrow f^5(A, J=5/2) + f^6(B, J=0)$

huge reduction factors to the one-electron 4f band width !!!